



THESIS  
2  
2004  
56611912

**LIBRARY  
Michigan State  
University**

This is to certify that the  
dissertation entitled

**MATHEMATICAL MODELING OF STATIC LONG-TERM  
STORAGE OF CORRUGATED BOXES**

presented by

**Manoch Srinangyam**

has been accepted towards fulfillment  
of the requirements for the

Ph.D. degree in Packaging



Major Professor's Signature

December 2, 2003

Date

**PLACE IN RETURN BOX** to remove this checkout from your record.  
**TO AVOID FINES** return on or before date due.  
**MAY BE RECALLED** with earlier due date if requested.

DATE DUE	DATE DUE	DATE DUE
01 06 10		
DEC 18 2005		
JAN 20 2011 08 17 10		

**MATHEMATICAL MODELING OF STATIC LONG-TERM STORAGE OF  
CORRUGATED BOXES**

**By**

**Manoch Srinangyam**

**A DISSERTATION**

**Submitted to  
Michigan State University  
in partial fulfillment of the requirements  
for the degree of**

**DOCTOR OF PHILOSOPHY**

**School of Packaging**

**2003**

## **ABSTRACT**

### **MATHEMATICAL MODELING OF STATIC LONG-TERM STORAGE OF CORRUGATED BOXES**

By

**Manoch Srinangyam**

The compression strength of a corrugated container is used to indicate the amount of top load that the corrugated container can withstand. This can be done by performing the standard test procedure, ASTM D 642. During long-term storage, the strength of a corrugated box will be substantially reduced over time. The corrugated container life can be determined by applying empirical strength retention factors obtained from published data. However, most published data is from decades ago and is questionable since the board making process and the content of paper has been changed significantly since then, especially due to the increased use of recycled paper. The accuracy of strength retention factors from published data was checked by placing dead loads on top of corrugated boxes. The time it took for the boxes to collapse was investigated. The results show that these published strength retention factors greatly overestimate box endurance. A new method for predicting failure times based on a mathematical model is presented here. The new test method uses a compression tester to compress a test box at a constant load level equal to a fraction of the ASTM D 642 compression strength. The deflection due to creep was recorded over a 12-hour

time period, which is a realistic limit for industry practice. A mathematical model was built based on engineering failure analysis. The results show a marked improvement in predictability using this method. The results also support the fact that corrugated boxes collapse during long-term storage when they absorb a critical amount of energy.

*To my parents  
Thongbai and Payub Srinangyam*

## **ACKNOWLEDGEMENTS**

I would like to take this opportunity to express my sincere gratitude to many people who, in one way or another, contributed to the completion of this dissertation.

First, I would like to express my special sincere gratitude to Dr. Gary Burgess, who served as co-advisor and was very devoted to my research. I am grateful for his guidance, effort, encouragement, kindness and willingness to help me throughout the research. Without him this research would not have been accomplished.

My sincere gratitude is also for my advisor, Dr. Bruce Harte. I am grateful for his patient, guidance, kindness and support. In addition, I would like to thank Dr. Paul Singh and Dr. Daniel Guyer for their advice, comments and great support throughout this research, and for serving as my committee members.

My special thanks is for the Thai Government for its financial support and giving me an opportunity to pursue my graduate studies in the United States of America.

I am thankful to Brett Rouyet at Kelloggs Company and David Filson at Clorox Company.

My warmest feeling goes to my great landlady, Mrs. Margaret Timnick, who makes me feel like staying back home in Thailand. I greatly appreciate her love, support, kindness and friendship. I would also like to extend my warmest feeling to Sukasem Sittipod and his family, Cengiz Caner, Youn Suk Lee,

Supachai Pisuchpen, Jay Singh and Bob Hurwitz for their friendships while I studied at MSU.

My heart felt thankful to my best friends, Chartchai Leenawong and Pronrudee Netisopakul, as well as to my girlfriend, Boonjeera Chiravate, for their constant love, care and support.

Last but not least, I would like to give very special thanks and gratitude to my family and my late aunt, Thongyib Thonglumjeag, for their endless love, care, support and encouragement on my education. Particularly, my parents, Thongbai and Payub Srinangyam, who are poor farmers, and have worked very hard in order to send me and their children to school. This feeling and appreciation is beyond any words to express and will be in my mind forever.

## TABLE OF CONTENTS

LIST OF TABLES .....	viii
LIST OF FIGURES .....	xi
1. INTRODUCTION .....	1
2. LITERATURE REVIEW .....	10
3. MATERIALS AND METHODS .....	32
4. RESULTS.....	44
5. DISCUSSION.....	58
6. CONCLUSIONS.....	102
APPENDICES .....	105
BIBLIOGRAPHY .....	138

## LIST OF TABLES

Table	Page
1.1 Time to collapse under constant load .....	3
1.2 Actual versus predicted times to fail at various top loads for box A.....	6
1.3 Actual versus predicted times to fail at various top loads for box B.....	6
2.1 Dimensional characteristics of common corrugated board.....	12
3.1 Specifications for boxes A and B used in this research.....	34
4.1 Compression strength and failure deflection of box A at various conditions.....	49
4.2 Compression strength and failure deflection of box B at various conditions.....	49
4.3 Deflection versus time at various constant loads for box A at standard conditions.....	52
4.4 Deflection versus time at various constant loads for box A at 80°F, 80%RH.....	53
4.5 Deflection versus time at various constant loads for box B at standard conditions.....	54
4.6 Deflection versus time at various constant loads for box B at 80°F, 80%RH.....	55
4.7 Actual times to fail of box A at various constant top loads and storage conditions.....	56
4.8 Actual times to fail of box B at various constant top loads and storage conditions.....	56
5.1 Deflection versus time under load for box A under constant load equal to 80% of ASTM D 642 at standard conditions.....	61

Table	Page
5.2 Deflection versus time under load for box A under constant load equal to 80% of ASTM D 642 at 80°F, 80%RH .....	62
5.3 Deflection versus time under load for box B under constant load equal to 80% of ASTM D 642 at standard conditions.....	63
5.4 Deflection versus time under load for box B under constant load equal to 80% of ASTM D 642 at 80°F, 80%RH.....	64
5.5 Creep rate, predicted and actual times to fail at various constant loads for box A at standard conditions.....	74
5.6 Creep rate, predicted and actual times to fail at various constant loads for box A at 80°F, 80%RH.....	74
5.7 Creep rate, predicted and actual times to fail at various constant loads for box B at standard conditions.....	75
5.8 Creep rate, predicted and actual times to fail at various constant loads for box B at 80°F, 80%RH.....	75
5.9 Creep rate, predicted and actual times to fail at various constant loads for box A at standard conditions.....	86
5.10 Creep rate, predicted and actual times to fail at various constant loads for box A at 80°F, 80%RH.....	86
5.11 Creep rate, predicted and actual times to fail at various constant loads for box B at standard conditions.....	87
5.12 Creep rate, predicted and actual times to fail at various constant loads for box B at 80°F, 80%RH.....	87
5.13 Corrected creep rates, predicted and actual times to fail of box A at standard conditions.....	92
5.14 Corrected creep rates, predicted and actual times to fail of box A at 80°F, 80%RH.....	93
5.15 Corrected creep rates, predicted and actual times to fail of box B at standard conditions.....	94

<b>Table</b>	<b>Page</b>
5.16 Corrected creep rates, predicted and actual times to fail of box B at 80°F, 80%RH.....	95
5.17 ASTM D 642 of box A at standard conditions.....	98
5.18 Actual versus predicted times to fail at various constant top loads of box A at standard conditions.....	99

## LIST OF FIGURES

Figure	Page
1.1 Long-term compression test with dead load.....	5
2.1 Corrugated board.....	11
3.1 Top view of box A.....	33
3.2 Top view of box B.....	33
3.3 Lansmont compression tester model 152-30TTC.....	35
3.4 Experimental design.....	37
3.5 ASTM D 642 test apparatus.....	39
3.6 Dead load test setup.....	43
4.1 ASTM D 642 results for box A at standard conditions.....	45
4.2 ASTM D 642 results for box A at 80°F and 80%RH.....	46
4.3 ASTM D 642 results for box B at standard conditions.....	47
4.4 ASTM D 642 results for box B at 80°F and 80%RH.....	48
4.5 Graph of deflection versus time under load at various constant loads for box A at standard conditions.....	52
4.6 Graph of deflection versus time under load at various constant loads for box A at 80°F, 80%RH.....	53
4.7 Graph of deflection versus time under load at various constant loads for box B at standard conditions.....	54
4.8 Graph of deflection versus time under load at various constant loads for box B at 80°F, 80%RH.....	55
4.9 Dead load test.....	57

Figure	Page
5.1 Typical creep curve of corrugated boxes under constant load.....	59
5.2 Creep of box A under constant load equal to 80% of ASTM D 642 at standard conditions.....	61
5.3 Creep of box A under constant load equal to 80% of ASTM D 642 at 80°F, 80%RH.....	62
5.4 Creep of box B under constant load equal to 80% of ASTM D 642 at standard conditions.....	63
5.5 Creep of box B under constant Load equal to 80% of ASTM D 642 at 80°F, 80%RH.....	64
5.6 ASTM D 642 curve.....	71
5.7 Typical graph between force and deflection obtaining from ASTM D 642.....	80
5.8 Graph between force and deflection of linear material.....	82
5.9 Compression strength of box B at different locations along box diagonal following ASTM D642 using floating platen.....	97
A1 Spring in tension.....	108
A2 Dashpot in tension.....	109
A3 Viscoelastic material modeled by spring (Hookean solid) and dashpot (Newtonian fluid).....	110
A4 Maxwell model of corrugated box in long-term storage.....	111
A5 ASTM D 642 of Maxwell model.....	114
A6 Graph of deflection versus loading time at constant load plotted from Maxwell model.....	116
A7 Kelvin model of corrugated box in long-term storage.....	117
A8 ASTM D 642 of Kelvin model.....	118

<b>Figure</b>		<b>Page</b>
A9	Graph of deflection versus loading time at constant load plotted from Kelvin model.....	120
A10	Hybrid model representing long-term storage of corrugated box.....	122
A11	ASTM D642 of hybrid model.....	125
A12	Graph of deflection versus loading time at constant load plotted from hybrid model.....	128

## 1. INTRODUCTION

Static long-term storage of corrugated boxes stacked in a warehouse is very important since the product packed inside the boxes can be damaged either from the boxes collapsing or from contact between the product packaged inside the corrugated boxes and the top panel of the boxes due to creep. Contact between the product and the top panel of the boxes due to creep is quite dangerous to the product inside, especially compression sensitive products such as glasses, chinaware, light bulbs, etc. This kind of problem also occurs with plastic containers and cartons packed inside corrugated boxes.

It would be very useful to the corrugated industry if one could accurately predict safe storage time of corrugated boxes during stacking in a warehouse. This knowledge will help packaging engineers to design corrugated boxes for specific top loads and storage times, protect products from damage and also reduce waste of corrugated material.

The ability of a corrugated box to withstand load or compression forces on the top of it while stacking in a warehouse is determined by its compression strength. The compression strength of a corrugated box can be measured using a laboratory compression tester. Compression strength can be determined according to ASTM D 642 (ASTM Committee D-10, 2003), Standard Test Method for Determining Compressive Resistance of Shipping Containers, Components and Unit Loads. Basically, the compression tester has a top platen moving downward with a speed of 0.5 inches per minute to compress the test box, which

is placed on a very sturdy table. The relationship between force and deflection is plotted. The top platen moves downward to compress the box until the box collapses. The maximum force on the graph is taken to be the box compression strength, and the corresponding deflection is the failure deflection.

### **1.1 Industry standard practice and long-term storage published data**

It is important to note that ASTM D 642, compression strength applies only to new boxes. In fact, boxes weaken over time in a stack. Long-term storage reduces box compression strength. The longer the boxes are stacked, the weaker they are. Time under load has long been known to reduce compression strength of boxes. A number of long-term stacking tests were performed in the 1960's and 1970's (Guins 1981, Maltenfort 1989, Maltenfort 1996) to evaluate the loss of compression strength over time. Based on these studies, empirical load versus duration curves were developed for box designers to calculate the effect of long-term storage on stacking strength (Guins, 1981). Nowadays, it is an industry standard practice to evaluate the compression strength of boxes under long-term storage as follows:

1. Perform ASTM D 642 using the compression test machine. Take the peak force on the graph between force and deflection to be the box compression strength.

2. Use published data obtained from load versus duration curves (Maltenfort, 1996) to calculate the storage time at any given top load. Table 1.1 shows representative data. By using Table 1.1, it is important to note that the

warehouse climate conditions and the climate conditions while performing ASTM D 642 should be the same.

Load (% Compression Strength)	Time to Fail
45%	2.7 years
50%	1 year
60%	1 month
70%	2 days
75%	12 hours
100%	immediately

Table 1.1: Time to collapse under constant load

If for example a corrugated box has an ASTM D 642 compression strength of 1,000 lbs, a 600 lb load stacked on the top of the box would represent a 60% load. According to Table 1.1, if a 600 lb load is loaded onto the top of a box, the box should collapse in 1 month. Likewise, if a 500 lb load is left on top of the box, the box should collapse in 1 year. The question is whether the data in Table 1.1 is still applicable since the experiments that produced the data were done long ago. Since that time, corrugated board has changed significantly in many ways. Manufacturing methods have also changed, especially with respect to the use of recycled paper in corrugated board. The use of recycled paper content could make corrugated board much weaker than in the past.

## **1.2 Accuracy of published data**

In order to evaluate the accuracy of long-term storage using dated published data, production-run boxes were obtained from commercial box manufactures. The knocked-down boxes were shipped in protective cartons to the School of Packaging, Michigan State University. They were regular slotted containers. The box A had full flaps. The box B was designed to save corrugated board by shortening both the top and bottom flaps. This box B style results in a hole in the top and bottom surfaces. Standard conditions of 73°F and 50% relative humidity were used in this test. ASTM D 4332 (ASTM Committee D-10, 2003), Standard Practice for Conditioning Containers, Packages, or Packaging Components for Testing, describes the standard preconditioning procedure. The boxes were erected, taped and preconditioned before the compression tests.

To determine the compression strength of the boxes A and B, the standard compression test was performed following ASTM D 642.

To evaluate the predictions in Table 1.1, sand bags and lead bricks weighted to 20, 40, 60 and 80% of the ASTM D 642 compression strength were placed on top of  $\frac{3}{4}$ " thick plywood platforms and placed on top of individual boxes following ASTM D 4577 (ASTM Committee D-10, 2003), Standard Test Method for Compression Resistance of a Container Under Constant Load. The test setup is shown in Figure 1.1. The test boxes were placed on a thick plastic sheet on the floor of a room held at standard conditions to prevent moisture uptake from the floor. The boxes were evaluated periodically. The time it took for the individual boxes to collapse was recorded. The result showed that the published long-term

storage data done many years ago greatly overestimates endurance. Table 1.2 and Table 1.3 show the comparison between the predicted failure times using published data and the sand bag test results.



Figure 1.1: Long-term compression test with dead load

<b>% load of the ASTM D 642 compression strength</b>	<b>Actual Time</b>	<b>Predicted time (Published data)</b>
<b>20%</b>	<b>over 6 weeks</b>	<b>never</b>
<b>40%</b>	<b>14 days</b>	<b>over 2 years</b>
<b>60%</b>	<b>2 days</b>	<b>30 days</b>
<b>80%</b>	<b>0.5 hours</b>	<b>10 hours</b>

**Table 1.2: Actual versus predicted times to fail at various top loads for box A**

<b>% load of the ASTM D 642 compression strength</b>	<b>Actual Time</b>	<b>Predicted Time (Published data)</b>
<b>20%</b>	<b>over 6 weeks</b>	<b>never</b>
<b>40%</b>	<b>8 days</b>	<b>over 2 years</b>
<b>60%</b>	<b>3 days</b>	<b>30 days</b>
<b>80%</b>	<b>0.5 hours</b>	<b>10 hours</b>

**Table 1.3: Actual versus predicted times to fail at various top loads for box B**

### **1.3 More work needed**

Based on the inaccuracies of the published long-term storage data, more study is needed to improve the accuracy of long-term storage predictions.

From the 1950's through 1970's, there were a number of studies regarding the static long-term storage of corrugated boxes. Initially, box researchers were interested in predicting box compression strength from corrugated board properties, such as edge crush, flexural and bending stiffness. Later, they were very interested in predicting static long-term storage of corrugated boxes. However, no one really discovered what caused failure during stacking under long-term storage conditions.

In the 1980's and 1990's, research tended to relate to static long-term storage of corrugated boxes microscopically, based on stress and strain analysis, of box board and panels locally, not the whole box as in the earlier studies. Some papers were published using finite element analysis techniques to model and simulate behavior and characteristics of corrugated boxes (Pommier 1991, Rahman 1997, and Beldie 2001). However, most researchers stated that more work needed to be done in this area in order to understand the behavior of corrugated board and to improve the finite element model, meaning that finite element analysis might not work well for this type of study. This also might be because corrugated board basically doesn't consistently show any obvious engineering material properties (Guins, 1981).

The following failure theories are commonly used in engineering failure analysis (Hearn, 1985). This will be discussed in detail in Chapter 5. These theories are maximum stress, strain and strain energy failure criterion as follows:

1. **Maximum Stress Failure Criterion:** This theory proposes that the box fails whenever the load on top of it reaches some critical value. This level would necessarily be the ASTM D 642 compression strength.

2. **Maximum Strain Failure Criterion:** This theory proposes that the box fails whenever its deflection reaches some critical amount. This amount would necessarily be the ASTM D 642 failure deflection. This deflection corresponds to the peak force (compression strength).

3. **Maximum Strain Energy Failure Criterion:** This theory proposes that the box fails whenever the energy it absorbs reaches some critical amount. This amount would necessarily be equal to the energy that the box absorbs during compression testing according to ASTM D 642.

Based of these engineering failure criteria, the hypothesis of this research is that one of above criteria or their combination causes corrugated box failure during stacking in static long-term storage.

#### **1.4 Research objectives**

The objectives of this study were as follows:

1. To improve the accuracy of published data and the industry standard practice for predicting static long-term storage of corrugated boxes.
2. To investigate the main criterion that determines corrugated box failure during stacking in static long-term conditions.
3. To develop a new test method and mathematical model for predicting storage time of corrugated boxes during stacking in static long-term conditions.

## **2. LITERATURE REVIEW**

### **2.1 Corrugated Board**

Corrugated board first appeared in 1856 in England, when a patent was granted to Healey and Allen for the first known use of corrugated paper instead of plain paper as a cushioning or lining for sweatbands of hats. In America, corrugated board was first used and patented by Albert L. Jones for packing lamp chimneys, glass bottles and fragile products in 1871 (Fibre Box Association, 1994).

The use of corrugated board has increased dramatically since World War II. More than 90 percent of all products in the United States are shipped in corrugated boxes (Miller, 2002). Corrugated fiberboard combines structural and cushioning characteristics needed for shipping lightweight containers at a low price. Corrugated packaging accounts for the largest segment of the packaging industry, with more than 1,600 plants mostly on the West and East coasts producing corrugated board and containers.

Corrugated board is composed of several layers of paper. The inner layer is called the corrugated medium. It is packed between two flat outer sheets called liners. The corrugated medium is connected to the two flat outer liners with glue as shown in Figure 2.1. This is called single wall corrugated board. Single face corrugated board can be laminated single wall to make a double wall corrugated board and so on. All the boxes to be used in this research are made from single wall corrugated board; it is also the most widely used corrugated board.

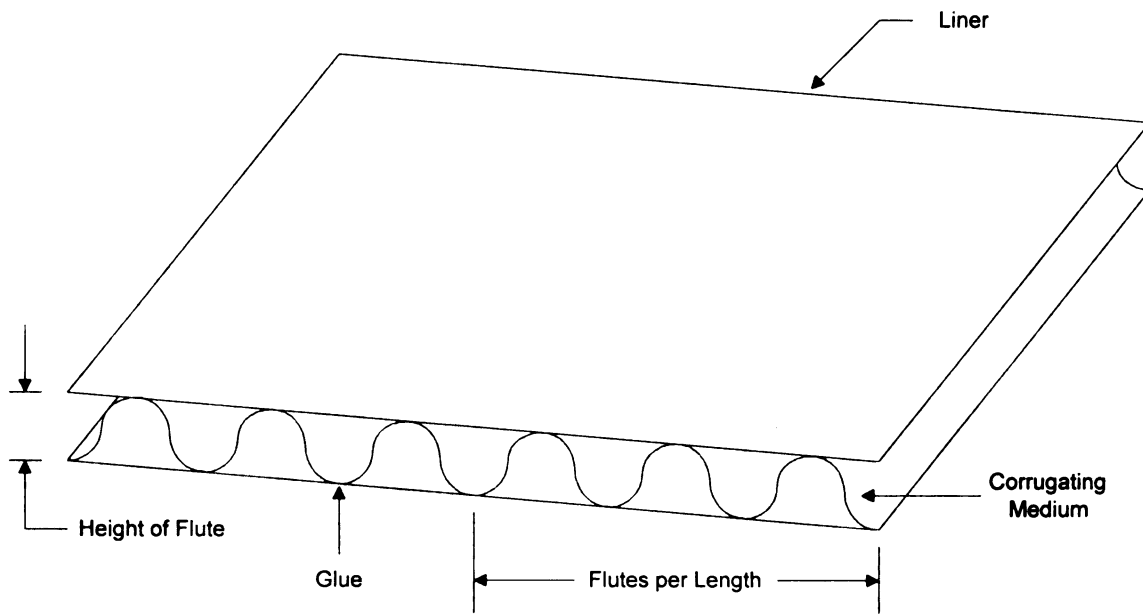


Figure 2.1: Corrugated board

Table 2.1 below shows the dimensional characteristics of commonly used corrugated board.

Board Type	Flutes per length (per ft)	Approximate Height (in)	Take up factor
A-flute	33±3	0.184	1.54
B-flute	47±3	0.097	1.32
C-flute	39±3	0.142	1.43
E-flute	90±4	0.062	1.27
F-flute	96±4	0.045	1.23

Table 2.1: Dimensional characteristics of common corrugated board

There are four main factors that control the structural performance of corrugated boxes (Guins, 1981).

1. Quality of the paper – characterized by fiber structure as produced by different pulping processes and also its basis weight.
2. Height of the flute
3. Number of flutes per unit length
4. Integrity of flute connection to the liners. The quality of glue also plays an important role.

## **2.2 Carrier Regulations**

Corrugated boxes can be used to ship a product by truck, railroad and air, or by a combination of these. The carriers want to make sure that the product will not get damaged during transportation. Proper shipping and handling can be done by using only corrugated boxes that meet Item 222 and Rule 41 (Fibre Box Association, 1994). Item 222 and Rule 41 are published and regulated by the National Motor Freight Traffic Association and the National Railroad Freight Committee, respectively. A box that follows the rules must have a circular marker called a box manufacturer's certificate (BMC) on the bottom flat of the box. The certified boxes must meet or exceed the minimum bursting test and combined basis weight, or the minimum edge crush test per the appropriate weight and dimensions of shipped product listed in Item 222 and Rule 41.

One might question which value is better to specify on a certified box: burst test or edge crush test. The answer is that it depends on what kind of environment the package will experience during shipment. If the package is expected to get a high compressive load on it, then use the edge crush test value on the box manufacturer's certificate. On the other hand, if the package is expected to contact or hit against the side walls of boxes, use the burst test value on the box manufacturer's certificate. Basically, packages that are shipped by small parcel service carriers, for example, United Parcel Service (UPS), Federal Express (FedEx) and the United State Postal Service (USPS) will encounter puncture hazard rather than high compressive loads. Simply speaking, the burst

test value is more important whenever puncture resistance is more critical than stacking strength or rough handling during transportation.

It is interesting to note that there is no relationship between the burst test value and compressive strength value of the corrugated board. For instance, if cloth is used for the liner of corrugated board instead of paper, the burst test value would be very high compared to the paper liner but the ability of the corrugated board to support a load would be negligible.

### **2.3 Stacking Strength**

Stacking strength is the amount of load that a box can support under actual use conditions. This is different from compression strength, which is the amount of load obtained from a compression tester under standard conditions following the ASTM D 642 test method in a laboratory. The stacking strength is less than the compression strength because the box may experience high humidity, long-term storage, stacking misalignment, interlocked pattern, pallet overhang and vibration during transportation (Fibre Box Association, 1994). All of the above factors can together reduce the ability of a box to withstand load, and the stacking strength value could be six times lower than the compression strength value.

## **2.4 Previous Work**

Much of the research related to corrugated board has been done by the Forest Products Laboratory of the United State Department of Agriculture, the Technical Association of the Pulp and Paper Industry (TAPPI), and by the Institute of Paper Science and Technology, formerly the Institute of Paper Chemistry. Carlson of the Forest Products Laboratory in 1939 was the first investigator to regard corrugated board as an engineering material (Maltenfort 1996). This resulted in study and evaluation of the properties of corrugated board as an engineering material. This suggests that the strength properties of the whole board can be correlated with the properties of the liners and corrugating medium. However, it is still very difficult to apply engineering theory to corrugated board as with steel or aluminum (Guins, 1981). There are two main reasons. First, engineers define engineering materials as substances having consistent characteristics over the whole material and their properties do not vary from batch to batch. Therefore, the concept of engineering design constants, for example, the modulus of elasticity, could be used for such representative groups as steel or aluminum as a whole. On the other hand, corrugated board properties can be different due to variations during production that result in varied performance of the corrugated board, even if those boxes are produced from the same batch of materials. The uniformity of the adhesive between corrugating medium and facing liners is very difficult to control, and this greatly affects the performance of corrugated board. Because of this fact, common engineering practices and engineering theory are difficult to apply to corrugated board in

process design. Secondly, corrugated board can change dramatically as it experiences varying environmental conditions of common storage use.

Engineering materials are, however, very stable in terms of their properties and characteristics at relatively constant conditions.

#### **2.4.1 Previous work related to properties of corrugated board**

The need to find corrugated board properties from which box compression strength could be predicted interested paperboard packaging engineers in the early 1950's. The edgewise compression strength of the corrugated board is an important parameter since it has correlation with box failure in top load compression. In 1961, R.C. McKee, J.W. Gander and J.R. Wachuta from the Institute of Paper Chemistry (McKee, Gander, Wachuta, 1961) published a study describing a suitable combined board column crush test method " Edgewise Compression Strength of Corrugated Board". Presently, the edgewise compression strength is commonly called the edge crush test (ECT). In addition, this technique and method was then developed to be ASTM D 2808. In an actual test 200 lb series, A-flute corrugated board was cut into samples perpendicular to its flute direction at different heights. All samples were 3 inch long. The samples were compressed parallel to the flute direction. The graph between compression strength (lbs/in) and column height were plotted. McKee and his co-workers found that column strength diminished rapidly with increasing column height. Samples more than 2 inch high bent before they collapsed. This suggested that a short column test would be the appropriate test sample for finding edgewise

compression strength since short column samples better represented board structural characteristics.

A second parameter related to box compression strength is the flexural stiffness of the corrugated board. This property is also needed to develop a box compression strength estimation formula. Flexural stiffness is the ability to resist bending. In 1962, McKee, Gander and Wachuta published a study on the flexural stiffness of corrugated board (McKee, Gander, Wachuta, 1962). A, B and C flute corrugated board were studied. Corrugated board samples were cut into strips and tested for flexural stiffness values in both the machine direction and cross machine direction using both the three-point beam and four-point method (McKee, Gander, Wachuta, 1962). From this study, they concluded that the flexural stiffness value of corrugated board depends on the modulus of elasticity and caliper of the board. Therefore, A, B and C flute corrugated board made from the same material components and having the same dimensions would be different in flexural stiffness values. Comparing the three-point beam and four-point methods, the four-point method was considered to be the proper way to determine flexural stiffness rather than the three-point beam method because the four-point method does not involve shear effects. The test results obtained from the three-point beam method reflect both flexural stiffness and shear rigidity of the material, meaning that this test method underestimates the real flexural stiffness value of the corrugated board.

In 1963, McKee, Gander and Wachuta published a formula to predict compression strength of corrugated boxes at standard condition (73°F, 50%RH) (McKee, Gander, Wachuta, 1963). They showed that the compression strength of single wall corrugated boxes is a function of box perimeter (2 times length + 2 times width), the edge crush test value of the corrugated board (ECT), and the flexural stiffness in both the machine and cross machine directions of the corrugated board. They also showed that the flexural stiffness is not an easy parameter to obtain in a laboratory. Moreover, there were quite a few laboratories equipped with instruments that could be able to generate flexural stiffness data at that time. For these reasons, McKee and his co-workers extended their work to express the relationship between the flexural stiffness value and edge crush test value and board caliper. Hence, the flexural stiffness in the formula was substituted with edge crush test and board caliper that resulted in a simpler formula which was practical to use because the simplified formula used parameters that are both easier to obtain in the laboratory and easier to work with in calculations. The simplified formula, however, is less accurate than the original formula but the difference in predicted values of both formulas is not significant. The original equation to predict compression strength of corrugated boxes was as follows:

$$P = 2.028 \times P_m^{0.746} \times \sqrt{(D_x D_y)^{0.254}} \times Z^{0.492} \quad (2.1)$$

where:

P = Box compression strength (lbs)

$P_m$  = Edge crush test value (ECT, lbs/in)

$D_x$  = Flexural stiffness in machine direction (lb-in)

$D_y$  = Flexural Stiffness in cross machine direction (lb-in)

Z = Box perimeter (2 times length + 2 times width, inches)

It is very important to note that the above equation comes with the condition that the height of box must be equal to or greater than one seventh of the box perimeter. As mentioned before, due to complexity of the original equation, flexural stiffness was replaced with the edge crush test value and board caliper to make the original equation more practical. Flexural stiffness had a high correlation to the edge crush test value and square of board caliper. Thus, the original equation was modified as follows:

$$P = 5.87 \times P_m \times h^{0.508} Z^{0.492} \quad (2.2)$$

Since both exponents (0.508 and 0.492) in the above equation were close to 0.5, another simplification was possible. This resulted in a well-known formula to predict compression strength of corrugated boxes. It was developed by McKee and his co-workers and is commonly used in the corrugated industry as follows:

$$P = 5.87 \times P_m \times \sqrt{hZ} \quad (2.3)$$

where:

$P$  = Box compression strength (lbs)

$P_m$  = Edge crush test value (ECT, lbs/in)

$h$  = Board caliper (inches)

$Z$  = Box perimeter (2 times length + 2 times width, inches)

After McKee and his co-workers published the formula to predict compression strength of corrugated boxes, G.G. Maltenfort extended McKee's work by employing McKee's formula with compression strength data obtained from double wall corrugated boxes (Maltenfort 1963). Maltenfort found that McKee's formula could be used not only for compression strength predictions of single wall corrugated boxes, but also for the prediction of double wall corrugated boxes as well.

In 1964, J.S. Buchanan, J. Draper and G.W. Teague published a paper related to the box compression strength formula (Buchanan, Draper and Teague 1964). They pointed out that the edge crush test and bending stiffness of corrugated board were the only crucial values that had a major impact on box compression strength. These parameters were used to generate the box compression strength prediction formula as follows:

$$K = C \times E^{0.75} \times D^{0.25} \quad (2.4)$$

where:

K = Box compression strength per unit of box perimeter

(lbs/in)

C = Constant

E = Edge crush test value (ECT), (lbs/in)

D = Bending stiffness with flute lengthwise (in-lb)

This equation was similar to McKee's formula. Both equations relate compression strength to three parameters, edge crush, flexural stiffness in McKee's formula compared to bending stiffness in Buchanan's formula, and box perimeter in McKee's formula, comparable to the box compression strength unit (lbs per box perimeter) of Buchanan's formula. Second, both formulas had similar exponent values (0.746 and 0.75) for the edge crush test. Buchanan also found from his study that bending stiffness of corrugated board is proportional to the square of board caliper, thus mathematically Buchanan's formula had the same relationship (square root of board caliper) as McKee's formula. However, Buchanan's formula is not as widely used as McKee's formula because more laboratory work is needed to determine bending stiffness.

Koning investigated the effect of facing liners and corrugating medium to corrugated box compression strength (Koning, 1978). He determined stress-strain properties of the facing liners and corrugating medium, and then calculated the box compression strength using a theoretical model from his previous study (Koning, 1975). The results showed that the actual and predicted compression strength values were all within 12% of each other. He varied stress-strain

properties of facing liners and corrugating medium by varying their basis weight. He concluded that to improve box compression strength, it might be more efficient to add fiber to the corrugating medium rather than facing liners.

Kawanishi had predictions of compression strength of corrugated boxes of various styles including wrap-around boxes and board moisture contents (Kawanishi, 1989). As mentioned before, McKee's formula predicts compression strength of only regular slotted containers at standard conditions (73°F, 50%RH). By using multivariate analysis, compression strength of corrugated boxes was derived from their specifications, boxes styles and moisture contents in the board. The drawback of the equation was that there were many parameters compared with McKee's equation. He, however, claimed that his new equation was consistent with the experimental results.

#### **2.4.2 Previous work related to properties of corrugated containers**

Maltenfort published a study about the correlation of corrugated box dimensions to their compression strength (Maltenfort 1956). This publication was prior to McKee publishing his compression strength prediction formula for corrugated boxes. In this study, Maltenfort measured compression strength of regular slotted corrugated boxes of various length, width and depth dimensions at standard conditions. He found that for any given value of the depth dimension, compression strength of the boxes had a linear relationship with the box perimeter. This conclusion was in contradiction with McKee's formula. McKee's formula describes the relationship between compression strength and box perimeter as a parabolic function that is curvilinear, not linear. Maltenfort also concluded that the depth of box had a small effect on box compression strength. This statement corresponds well with McKee's, since he stated as a condition of use that the height of the box must be equal to or greater than one seventh of the box perimeter. This means that it does not matter what the height of the box is. The box compression strength would be slightly different or even the same value (at the same box perimeter) whenever the height of the box is equal to or greater than one seventh of the box perimeter.

Kellicutt from the Forest Products Laboratory of the United States Department of Agriculture, Madison, Wisconsin, studied the effect of contents and load bearing surface on the compression strength and stacking life of corrugated containers (Kellicutt 1962). Boxes made from the same material and perimeter but different depths were used. Compression tests were done on

sample boxes until they failed. He discovered that for shallow boxes, failure resulted almost totally by crushing along the top and bottom horizontal score lines. As the box height increased, failure resulted from crushing along top and bottom horizontal score lines and buckling of the box panels. Buckling of the box panels could be both inward and outward. In general, two bow inward and two outward. For a very tall box, failure comes entirely from buckling of box panels. In the second part, the same kinds of boxes were perfectly aligned in a stack three high and compressed using a compression tester. The results showed that compression strength of the stacked boxes was about 23% less than in individual box tests. He reasoned that because the top surface of the top box and the bottom of the bottom box were perfectly parallel, there was smooth contact with the platens of the compression tester. Conversely, the other top and bottom surfaces of the boxes in the stack were loaded unevenly on the top and bottom surfaces of neighboring boxes. He also showed that if the center box in the stack was intentionally placed  $\frac{1}{2}$ " out of alignment, the compression strength was decreased to 50% of the individual box test. This reduction occurred because the box corners were misaligned. Hence, the top corners of the bottom box and the bottom corners of the top box made contact in some places on the flaps of the middle box instead of its corner, which is the stiffest part of the box.

Furthermore, Kellicutt showed that an interlocked pattern of corrugated boxes stacked on a pallet reduced box compression strength to 55%. The third phase of his work investigated the effects of the contents in the box on box compression strength. The same boxes were filled three different ways: one was

filled with shelled corn, one had four pieces of plywood 2" below the top to restrict all four panels from bowing inward, and one was empty. The results showed that boxes containing shelled corn and plywood insertion had compression strength slightly more than empty box, (about 8%). He reasoned that this was because the shelled corn and the inserted plywood inside the boxes restricted the panels of the boxes from bowing inward, forcing the box panels to stand upright rather than bending inward to support the load. Kellicutt also showed that a dead load with 65% of the compression strength placed on an empty box caused failure in about 35 days. Boxes containing shelled corn with a dead load of 65% of compression strength could extend the duration to 43 days.

Kutt and Mithel studied the effects of bearing area and stress distribution applied on the top box panel (Kutt and Mithel 1969). They found that the compression strength of corrugated boxes decreased very extensively, when the bearing area was reduced. Moreover, they also found that the corners could resist tremendous amounts of load compared with the edges along the perimeter between the corners. They also claimed that just before the box failed, most of the load was transferred directly to the box corners. McKee stated that the four corners took about two thirds of the compression load (McKee, Gander, Wachuta, 1963).

Maltenfort examined the compression load distribution on corrugated boxes and the effect of asymmetrical board construction (Maltenfort, 1980). He found that the four corners of the corrugated box carried about 64 percent (two

thirds) of compression load; the edges along the perimeter between the corners carried the remaining 36 percent. This result was consistent with McKee study. In addition, Maltenfort examined the effect of asymmetrical board construction on compression strength, in particular, different basis weight of inside and outside liners using filled boxes. By using filled boxes, the buckling of panels was only outward. He found that the box with the thicker inside liner had slightly more compression strength than the box with thinner inside liner. He believed this was because the inside box panels were in compression, while the outside box panels were in tension. The thicker the inside box panels, the more compression they can withstand.

Peterson and Fox provided an explanation for how boxes fail in compression (Peterson and Fox, 1980). They treated corrugated materials as engineering structures. Based on the Rayleigh-Ritz approach, a mathematical model was been constructed. A photoelastic stress technique was also used to generate stress distribution patterns on the external surface of the box side panels, which were subjected to loading. The stress on the box panels was then calculated. They concluded that failure occurred when the stress state at any point on the box panel surface exceeded the failure criterion.

Moody and Skidmore investigated the creep characteristic of corrugated boxes when compressed underneath a dead load (Moody and Skidmore, 1966). They found that while the box was under dead load the relationship between box deflections and loading time could be divided into three creep regions. The primary creep region of compression time curve begins with the application of

load. The graph in this primary region was likely a curve rather than a straight line. Typically, primary creep happens during the first couple minutes of the compression. After that, the box deflection gradually increases with constant rate. This state is called the secondary creep region. This process could take days, months or years: depending on the amount of the dead load. Lastly, the deflection increases rapidly and the box fails at this state. This last state is called tertiary creep region. By making use of the information from either the primary creep region or the secondary creep region, they tried to predict long-term storage survival time. However, they were not successful.

Koning Jr. and Stern studied the long-term creep in corrugated fiberboard containers (Koning Jr. and Stern 1977). Subsequently, they drew a line illustrating the relationship between secondary creep rate per box depth and box survival time under dead load. They, therefore, proposed that the relationship between them is linear, under a log-log scale. The equation of this line is as follows:

$$T = \frac{4988}{R_{KS}^{1.038}} \quad (2.5)$$

where:

T = Duration of load or survival time (hour)

$R_{KS}$  = Secondary creep rate per box depth (in/in/hr x  $10^6$ )

It is important to note that Koning Jr. and Stern used secondary creep rate per box depth instead of actual secondary creep rate. However, the data from the experiment came from different flute types, adhesives and conditions to either

73°F, 50%RH or 80°F, 90%RH. Their research could be considered to be the first attempt to predict long-term storage survival time using short term-dead load tests.

Thielert published his study entitled determination of stacking load-stacking life relationship of corrugated cardboard containers (Thielert, 1984). A dead load of 90%, 80% and 60% of box compression strength was set to individual boxes. Ten replicates were tested at each percent load. The boxes were periodically investigated. The time it took for the individual boxes to collapse was measured. Accordingly, he found a linear relationship between the percent load and the logarithm of the boxes' median stacking survival time. Moreover, the distribution of stacking survival time was not normal. The result, therefore, demonstrated large variations. Consistently, these variations of experimental result were also reported by the previous studies of Moody and Skidmore (Moody and Skidmore, 1966) and Koning Jr. and Stern (Koning Jr. and Stern, 1977).

In 1986, Thielert studied the relationship between edgewise compression strength and long-term storage survival time of corrugated board (Thielert, 1986). By compressing corrugated boxes at different speeds, he found a straight-line relationship between compression strength and the logarithm of compression tester platen speed, which meant that compression strength of the box depended on the speed of the compressed platen. He tried to relate this linear relationship with long-term storage time, but the result was considerably different from his own previous work (Thielert, 1984). He finally concluded from his study that there

is no simple way to predict long-term storage survival time on the basis of the relationship between edgewise compression strength and compression speed.

Thorpe and Choi studied strain on panels of corrugated containers while loading using a technique called linear image strain analysis (LISA), which basically is a noncontact method for measuring strain fields in paper and paperboard (Thorpe and Choi 1991, Thorpe and Choi 1992). The LISA technique could, however, measure only two-dimensional and in-plane strains, while in fact, the deformation process occurs in three dimensions. They reported that the vertical panels maintained their integrity at strain value more than those that caused failure of individual linerboard specimens. The failure was associated with alternating normal shear strain near the vertical edges of the container. In addition, the failure occurred not only through degradation of corrugated board structural, but also by a gradual increase in out-of-plane bowing. This, finally, leads to collapse of the structure.

Pommier, Poustis, Fourcade and Morlier studied the critical load of a corrugated cardboard box submitted to vertical compression using finite elements methods (Pommier, Poustis, Fourcade and Morlier 1991). This could be regarded as the first published paper that proposed an alternative to predict box compression strength using finite element methods, rather than McKee's formula. To make the model simpler, a flapless corrugated container was modeled instead of regular slotted containers style. The linear theory was used. Based on linear theory, it was justified because in the loading process the deflection of corrugated box panels was substantial. They noted that the model still needed

verification from experiments and more information from observations on the inter-plate bond in corrugated board.

Rahman evaluated the buckling performance of corrugated board panels under compressive loading using finite element analysis (Rahman, 1997). In his study, the buckling analysis was used to determine the critical buckling stress that would result in the instability of the corrugated board components. The finite element model explained the behavior, the mechanism of the failure, and the role played by liners and corrugating medium in a buckling failure. An analysis of corrugated board panels representing a range of board stiffness which indicated that local buckling was dominant in components whose panels ratio (length/width) was lower than a determined threshold value. As the slenderness ratio increased, global buckling became more dominant. The buildup of shear stresses at the joints between liners and corrugated medium contributed to the local buckling failure.

Beldie, Sandberg and Sandberg studied the mechanical behavior of corrugated containers subjected to static compression loads using a finite element method (Beldie, Sandberg and Sandberg, 2001). The study was divided into three parts, and subsequently the results from experimental and finite element analysis were compared. First, a sheet of corrugated board was cut and subjected to compression testing. Secondly, a corrugated container was cut into segments and each segment was subjected to compression tests to determine the load contribution of each segment. Thirdly, the whole container was subjected to compression testing to see the overall performance of the container.

The result showed that the numerical computation of corrugated board subjected to compression load exhibited consistency with the test result. The consistency was, however, less when the height of the corrugated board decreased. They reasoned that because the local deformation of the edges had a significant influence on short corrugated board panels. Furthermore, they found that the middle segment of the container experiences a higher stiffness than that of the upper and lower container segments and that of the whole container. Subsequently, their conclusion was that the low initial stiffness of the container was a consequence of the low stiffness of the upper and lower corners, i.e. of the horizontal creases. The stiffness of corrugated board was dictated mostly by the creases. However, they noted that the creases were modeled as hinges in the finite element model. For these reasons, a more accurate model is called for. More work needs to be done in order to understand the behavior of the crease, and to improve the finite element model of a corrugated board container.

### **3. MATERIALS AND METHODS**

#### **3.1 Materials**

Two types of regular slotted containers were used in this research, boxes A and B. The box A has full flaps. The box B is designed to save some corrugated board by shortening both the top and bottom flaps. This box B style results in a hole in the top and bottom surfaces.

The box A was made by a box manufacturer which supplies boxes to a cereal manufacturer. The box A is shown in Figure 3.1. The box B was made by a box manufacturer which supplies boxes to a household chemical company. The box B is shown in Figure 3.2. The knocked-down boxes were shipped to the test facility at the School of Packaging, Michigan State University in protective cartons. The boxes were erected, taped and preconditioned before use. The box manufacturer's certificates, basis weight of corrugated board and dimensions of both boxes used in this research are described in Table 3.1.



Figure 3.1: Top view of box A



Figure 3.2: Top view of box B

Boxes	Board	Basis Weight (lb/1000ft <sup>2</sup> )	Dimensions (W x L x D)	Edge Crush Test (lb/in)	Size Limit (in)	Gross Wt Lt (lb)
A	B-Flute Single wall 0.125 " thick	44/28/44	15"x19.5"x12"	44 (45*)	95	95
B	C-Flute Single wall 0.175 " thick	48/30/48	13"x19.5"x10"	44 (51*)	95	95

\* Actual edge crush test values from laboratory

Table 3.1: Specifications for boxes A and B used in this research

### 3.2 Equipment

- Compression tester model 152-30TTC made by Lansmont Corporation  
(shown in Figure 3.3)
- Paper tape
- 4,000 lbs of 50 lb sand bags
- 1,000 lbs of 50 lb lead bars
- 48" x 32" x 3/4" plywood, 8 pieces
- Plastics bags
- Balance
- Ruler
- Conditioning room

### 3.3 Test Conditions

Two storage conditions were used in this study: a temperature of 73°F and 50% relative humidity (standard conditions), and a temperature of 80°F and 80% relative humidity. All box samples were conditioned for at least 72 hours at these conditions in accordance with ASTM D 4332 before any tests.

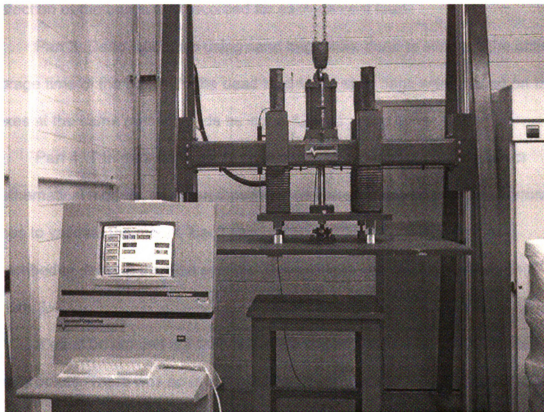


Figure 3.3: Lansmont compression tester model 152-30TTC

### **3.4 Methods**

In this research, the experimental design was divided into 4 parts.

Part 1: Both the boxes A and B were compression tested using ASTM D 642. The compression strengths and peak deflections were recorded for each box.

Part 2: 12-hour creep tests were done at 20%, 40%, 60% and 80% of the compression strength obtained from the ASTM D 642 tests. Time versus deflection of the boxes was recorded for each percent load.

Part 3: Dead load tests using sand bags were done to simulate the actual storage time of the boxes. In the dead load tests, sand bags were placed on the boxes at the same percent loads as in the 12-hour creep tests.

Part 4: The data from the 12-hour creep tests were used to construct mathematical models, and then those models were compared with actual storage times to validate the model. Each part of the experimental design will be described in detail in the next section. The experimental design is shown in Figure 3.4.

It must be pointed out that all sample boxes used in this research were empty boxes. There was no product inside. These, of course, are ideal conditions that make it easy to analyze the problem, but would not be expected to occur in real life. There are many kinds of products that require the box to carry the entire load, for example, glassware, chinaware, and light bulbs. Therefore, the results from this research do apply to these situations.

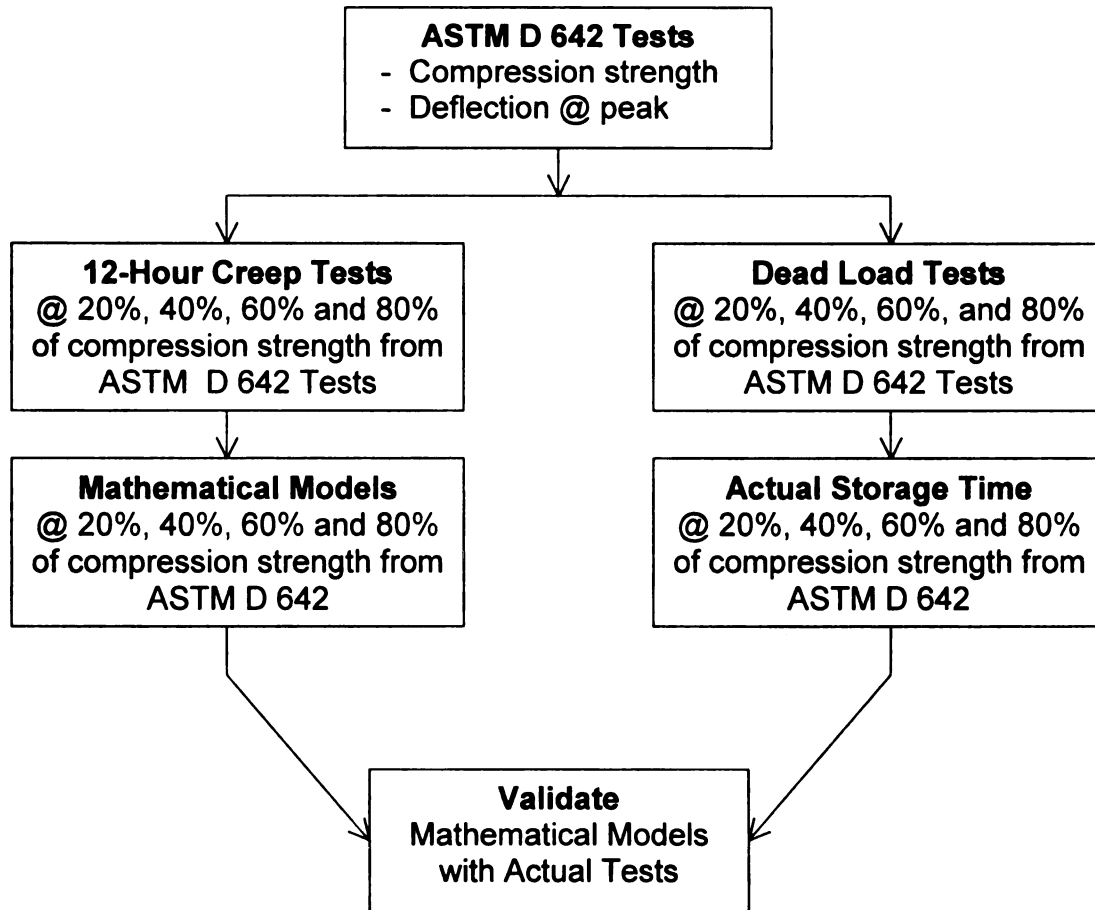


Figure 3.4: Experimental design

### **3.4.1 ASTM D 642 Tests**

ASTM D 642 (ASTM committee D-10, 2003), Standard Test Method for Determining Compressive Resistance of Shipping Containers, Components, and Unit Loads, was used in this study to obtain box compression strength and also box deflection at peak force. All box samples were preconditioned in accordance with ASTM D 4332 before compression testing. Each test box was placed in a sealed plastic bag to maintain moisture content of corrugated board. Each test box in the sealed plastic bag was placed inside the compression tester between the upper moving platen and the fixed metal table. Fixed platen testing and a 50 lb preload was used for these tests. A 50 lb preload is suggested for single wall corrugated board in order to make sure that all four corners of the box contact the platen. Box deflection was measured from this point. The moving platen moved downward at a constant speed of 0.5 inches per minute. The compression force increased until it reached its maximum value, which defines the box compression strength. The box deflection at peak was also recorded. At this moment, the box collapsed and completely lost its compression strength. The compression force decreased with increasing box deflection after peak. Eventually, the compression tester stops when the applied force drops to 75% of the compression strength value. The relationship between compression force and box deflection was then graphed. The ASTM D 642 test apparatus is shown in Figure 3.5.

Five replicates were tested for boxes A and B, and at each test condition. The compression strength values from the five replicates were then averaged.

The average compression strength values were used to determine the weight to apply to the test boxes for the 12-hour creep tests and the dead load tests.

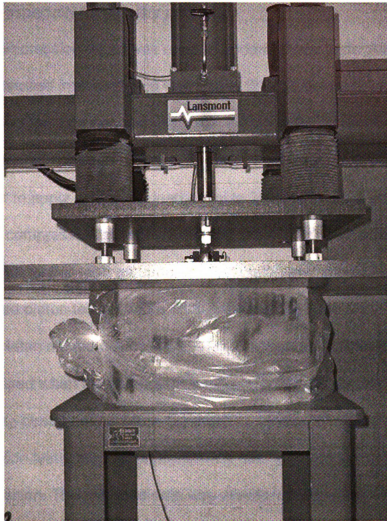


Figure 3.5: ASTM D 642 test apparatus

### **3.4.2 12-Hour Creep Tests**

The 12-hour creep tests were designed to obtain data in order to construct mathematical models that allowed the 12-hour creep test results to be extrapolated to failure. There is a reason for these tests. The 12 hours test is a realistic limit, especially for industry practice.

The compression tester was used to perform these tests. All box samples were preconditioned in accordance with ASTM D 4332 before doing the 12-hour creep tests. The test box was also placed in a sealed plastic bag to maintain moisture content of corrugated board. To perform creep tests, the compression tester was set to apply a constant load equal to 20%, 40%, 60% and 80% of the ASTM D 642 compression strength. Each test box was placed inside the compression tester between an upper moving platen and a fixed metal table at the base. Fixed platen testing and a 50 lb preload were used for all these tests. The moving platen moved downward at a constant speed of 0.5 inch per minute, and then stopped when the compression force reached the desired value. After a 12-hour testing period during which the machine measured deflection over time, the compression tester stopped automatically, and then the platen moved up to its original position. The recorded data was printed out and showed the relationship between box deflection over time. The setup for the 12-hour creep test is as same as the ASTM D 642 as shown in Figure 3.5. The difference is that for the 12-hour creep test, when the compression load reaches a present amount, the compression tester maintains the load level for 12 hours.

Five replicates were tested for boxes A and B, at each test condition, and also for each percent load (20%, 40%, 60% and 80%) from ASTM D 642. The data from the five replicates were then averaged. The averaged data was then fitted into mathematical models.

### **3.4.3 Dead Load Tests**

To achieve the actual failure times for long-term storage of corrugated boxes, dead load tests were designed to present real life conditions on a laboratory scale.

All box samples were preconditioned in accordance with ASTM D 4332 before dead loading; 50 lb sand bags were used as the dead load since it is an inexpensive material; 50 lb lead bars were also employed as the dead load. The dead loads were set at 20%, 40%, 60% and 80% of the ASTM D 642 strength. The test boxes were placed on a thick plastic sheet on the floor of a conditioning room to prevent moisture uptake from the floor. A piece of plywood 40" x 32" x 3/4" was placed on top of the test boxes. The sand bags and lead bars were carefully placed and centered on top of the plywood. A 50 lb preload was also applied for the dead load tests. The sand bags and lead bars were then loaded on top of plywood until the desired load was achieved.

In practice, the plywood does not move downward evenly, meaning that all four corners of the test box do not deflect the same distance. The four corners of the test boxes show different deflections because the center of gravity of the dead load is never over the center of the test box. The dead load setup is shown

in Figure 3.6. The off-centered load resulted in the tilting of the four corners. This causes differences in height of each corner. However, these corner heights were not significantly different since the sand bags were carefully positioned on the plywood so that the center of gravity of the sand bags was located precisely over the center of the test box.

Two replicates were tested for boxes A and B, at each test condition, and also for each percent load (20%, 40%, 60% and 80%). The test boxes were checked for failure every half an hour for the first 6 hours and every day thereafter. The time it took for the individual boxes to collapse was recorded. The data from the two replicates were then averaged. The averaged data was then compared with the mathematical models.



Figure 3.6: Dead load test setup

## **4. RESULTS**

### **4.1 ASTM D 642 Tests**

The graphs of force and deflection (ASTM D 642) for boxes A and B at standard conditions and 80°F, 80%RH are shown in Figures 4.1, 4.2, 4.3 and 4.4. These graphs are averages over five replicates. The compression strength and failure deflection are shown in Tables 4.1 and 4.2.

Peak force = 730 lbs, Deflection at peak = 0.28 inch

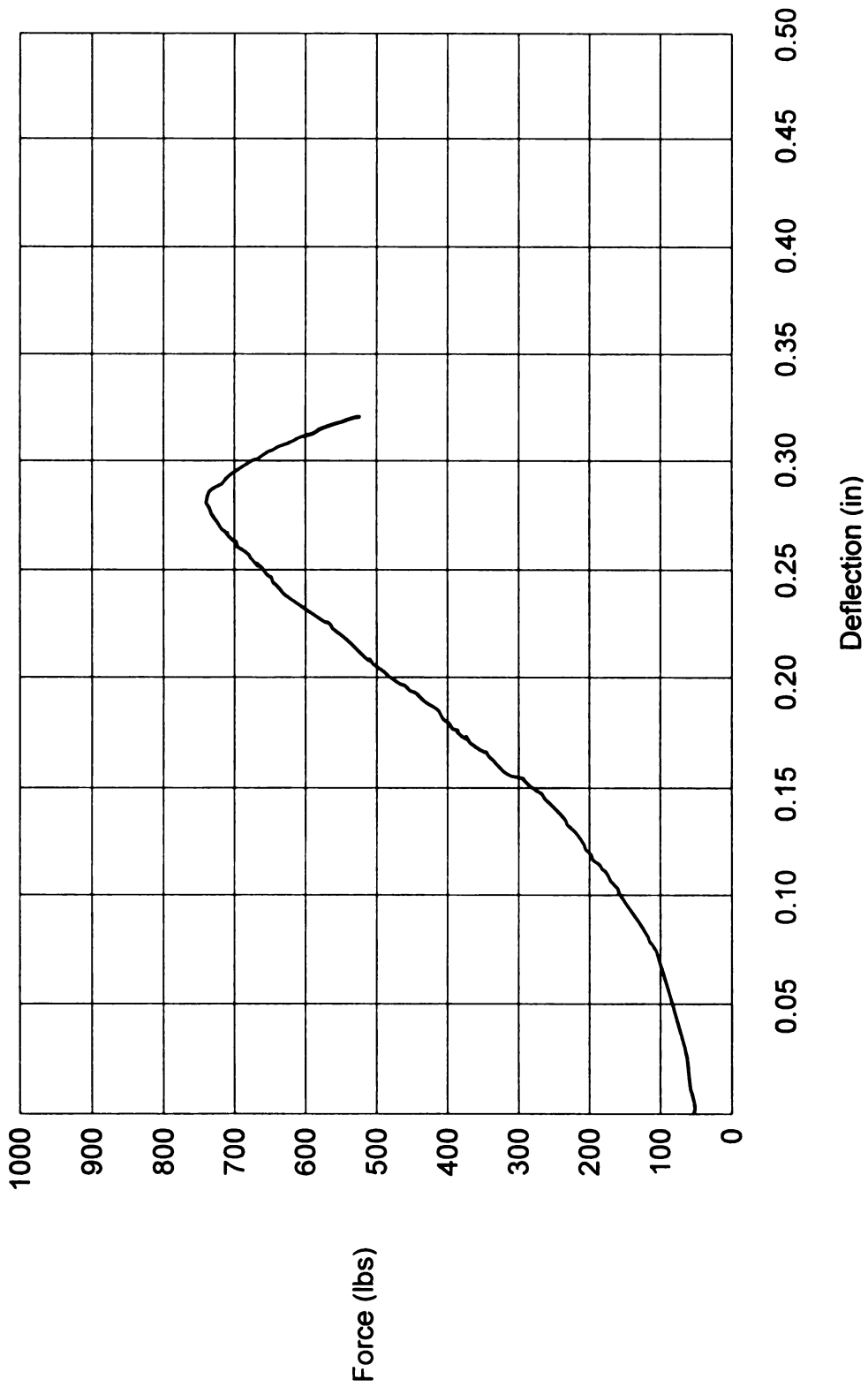


Figure 4.1: ASTM D 642 results for box A at standard conditions

Peak force = 595 lbs, Deflection at peak = 0.25 inch

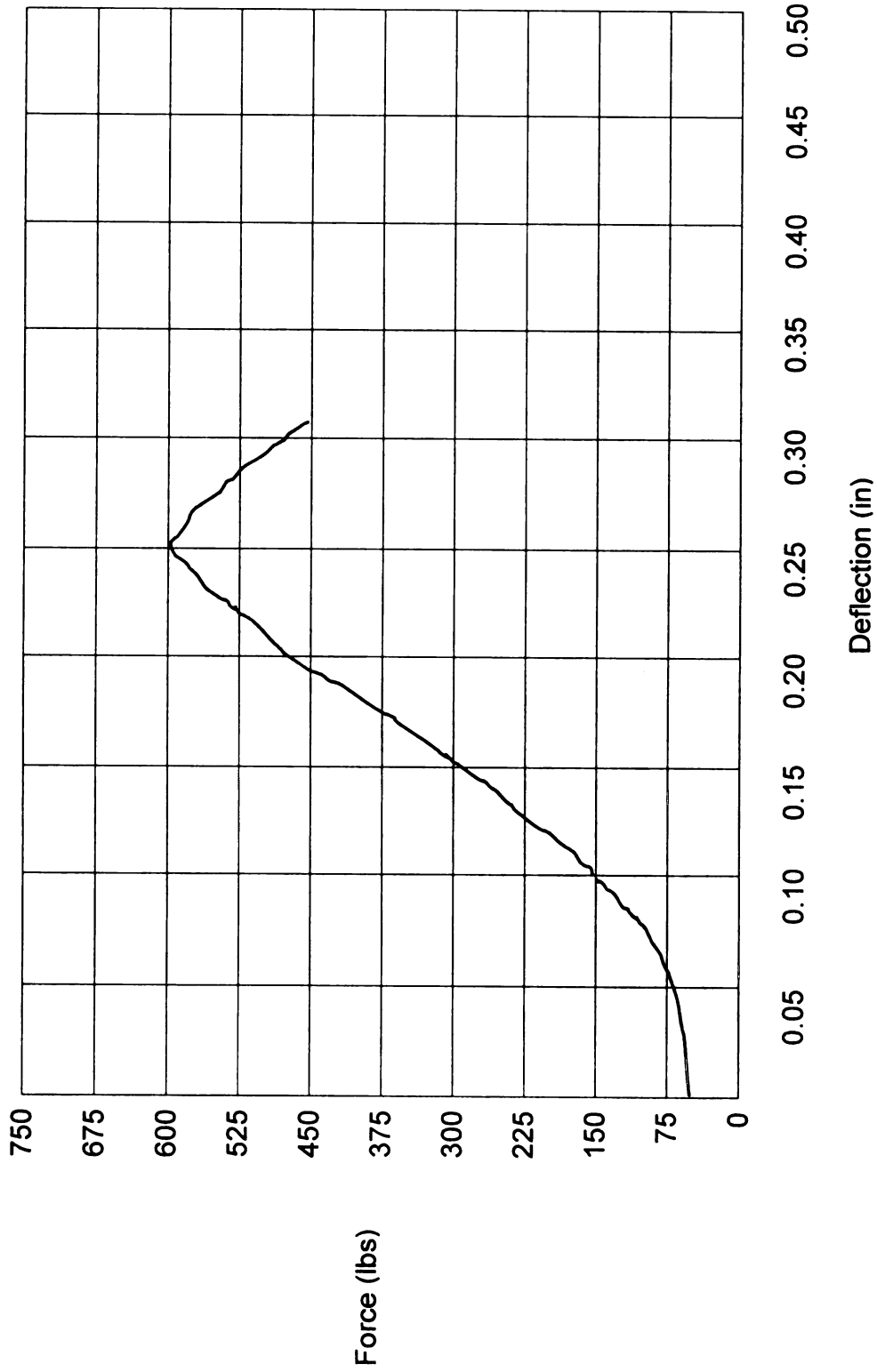


Figure 4.2: ASTM D 642 results for box A at 80°F and 80%RH

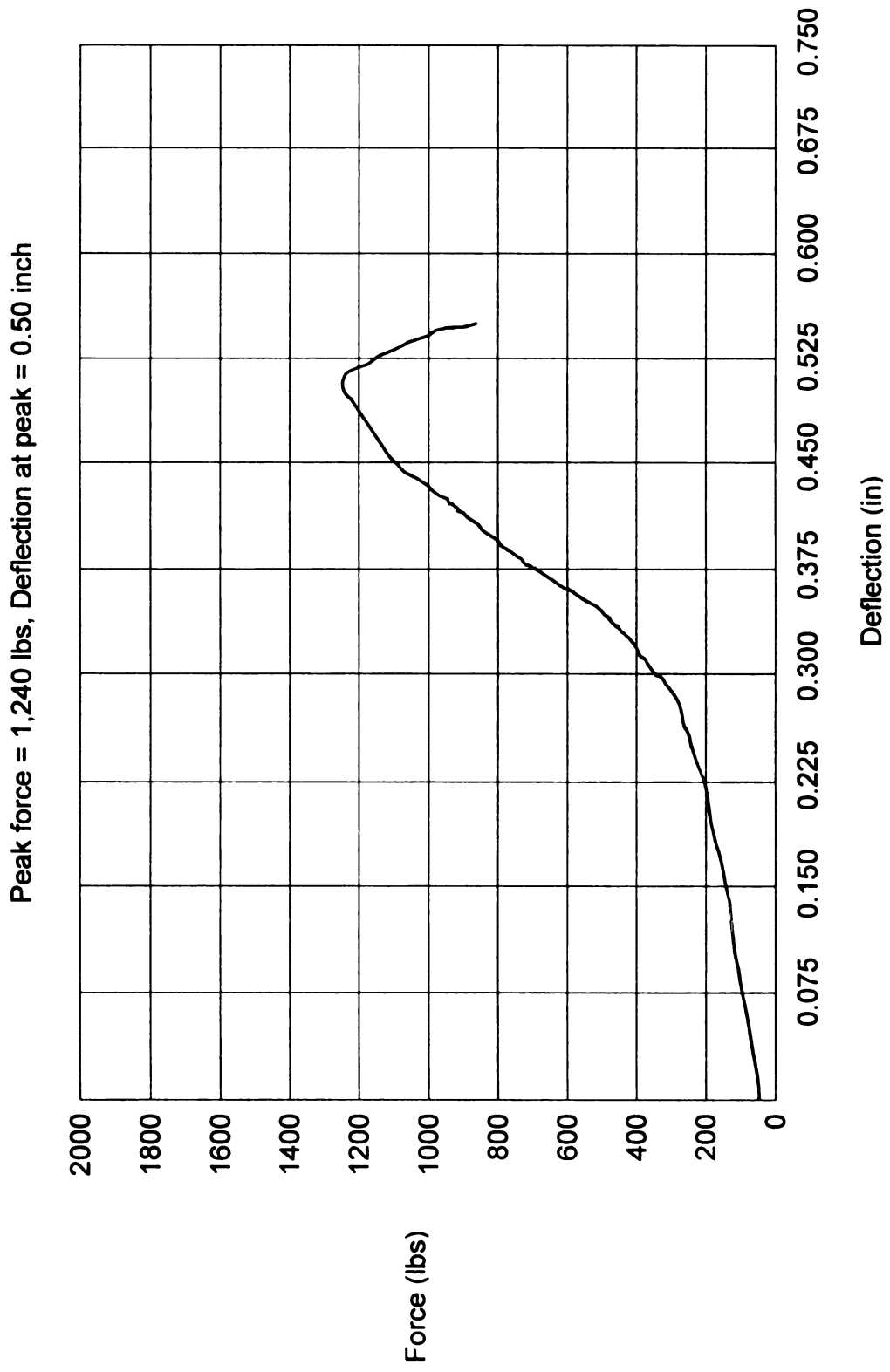


Figure 4.3: ASTM D 642 results for box B at standard conditions

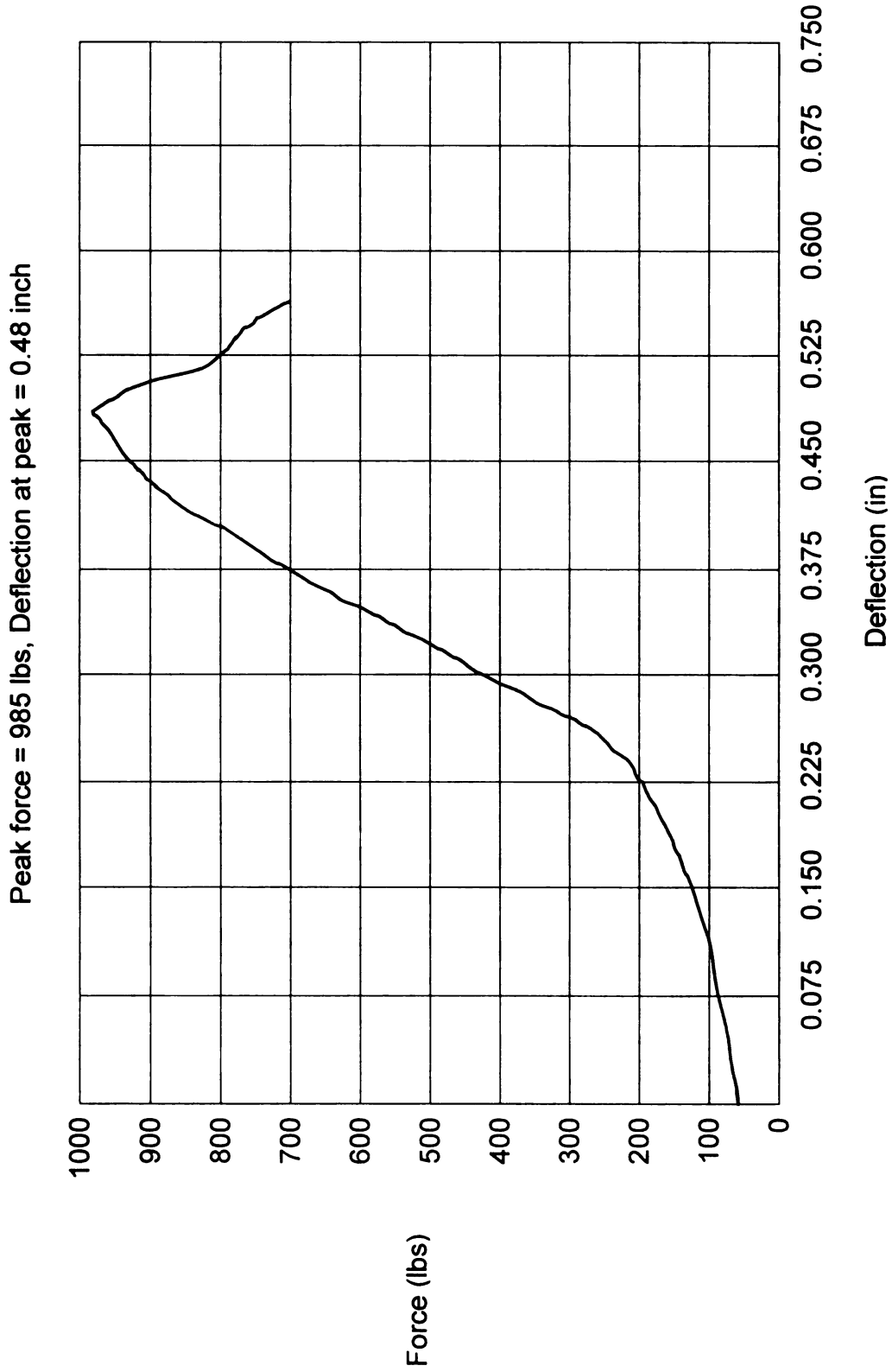


Figure 4.4: ASTM D 642 results for box B at 80°F and 80%RH

Storage Condition	Compression Strength (lbs)	Failure Deflection (in)
Standard (73°F, 50%RH)	730	0.28
80°F, 50%RH	595	0.25

**Table 4.1: Compression strength and failure deflection of box A at various conditions**

Storage Condition	Compression Strength (lbs)	Failure Deflection (in)
Standard (73°F, 50%RH)	1,240	0.50
80°F, 50%RH	985	0.48

**Table 4.2: Compression strength and failure deflection of box B at various conditions**

According to Tables 4.1 and 4.2, the compression strength of boxes A and B was 730 lbs @ 0.28 inch and 1,240 lbs @ 0.50 inch at standard conditions respectively.

By applying McKee's formula as shown in Eq. (2.3), and using the board information shown in Table 3.1, box compression values were predicted at standard conditions. The calculated compression strengths are

$[5.87 \times 45 \times \sqrt{(0.125)(69)}] = 775$  lbs and  $[5.87 \times 51 \times \sqrt{(0.175)(65)}] = 1,010$  lbs for boxes A and B, respectively. The result shows that McKee's formula can predict

compression strength of box A with only about  $\frac{(775 - 730)}{730} \times 100 = 6\%$  error, but

$\frac{(1,240 - 1,010)}{1,240} \times 100 = 18\%$  for the box B. It is noted that instead of using edge

crush test values from box manufacturer's certificates, the actual edge crush test values from laboratory analysis were used to calculate the compression strength in McKee's formula. This is because the edge crush test values from laboratory testing represent the actual corrugated board properties.

## **4.2 12-Hour Creep Tests**

The box deflection versus time under load at loads equal to 20%, 40%, 60% and 80% of the ASTM D 642 compression strength of boxes A and B at standard conditions and 80°F, 50%RH are shown in Tables 4.3, 4.4, 4.5 and 4.6. These box deflections are averages over five replicates. The tabular results are graphed as shown in Figures 4.5, 4.6, 4.7 and 4.8.

Time (min)	Deflection @ 20% CS (in)	Deflection @ 40% CS (in)	Deflection @ 60% CS (in)	Deflection @ 80% CS (in)
0	0	0	0	0
1	0.110	0.146	0.198	0.228
2	0.114	0.152	0.200	0.240
4	0.114	0.152	0.206	0.248
8	0.116	0.154	0.212	0.258
16	0.116	0.160	0.212	0.262
32	0.116	0.160	0.212	0.278
64	0.118	0.162	0.214	0.280
128	0.120	0.164	0.222	0.280
256	0.126	0.166	0.222	Failed
512	0.126	0.168	0.224	Failed
720	0.126	0.168	0.230	Failed

Table 4.3: Deflection versus time at various constant loads for box A at standard conditions

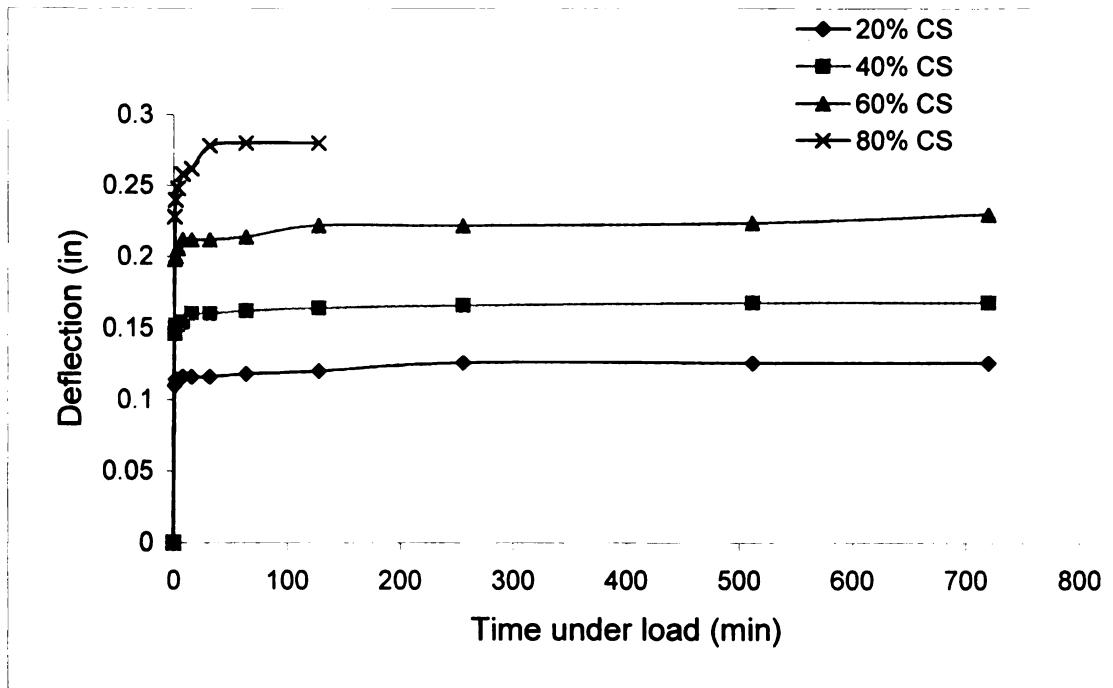


Figure 4.5: Graph of deflection versus time under load at various constant loads for box A at standard conditions

Time (min)	Deflection @ 20% CS (in)	Deflection @ 40% CS (in)	Deflection @ 60% CS (in)	Deflection @ 80% CS (in)
0	0	0	0	0
1	0.124	0.150	0.190	0.220
2	0.130	0.152	0.196	0.234
4	0.132	0.154	0.200	0.244
8	0.134	0.160	0.204	0.250
16	0.138	0.160	0.206	0.250
32	0.138	0.162	0.208	Failed
64	0.140	0.166	0.208	Failed
128	0.144	0.166	0.210	Failed
256	0.146	0.168	0.216	Failed
512	0.146	0.170	0.220	Failed
720	0.148	0.172	0.224	Failed

Table 4.4: Deflection versus time at various constant loads for box A at 80°F, 80%RH

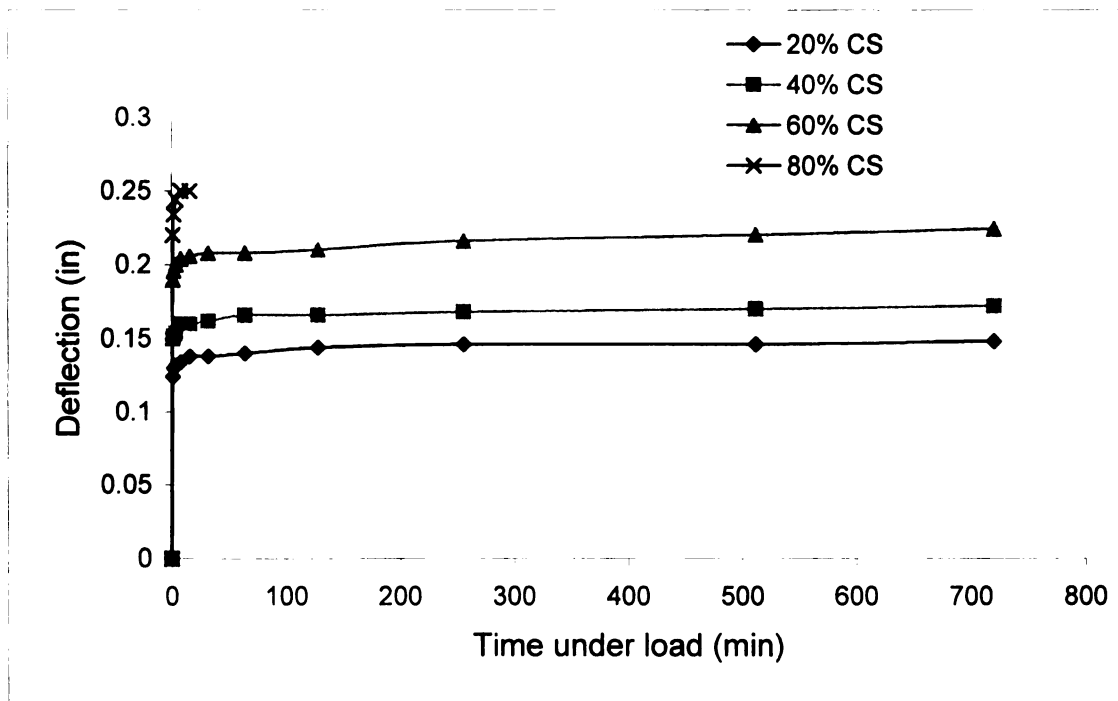


Figure 4.6: Graph of deflection versus time under load at various constant loads for box A at 80°F, 80%RH

Time (min)	Deflection @ 20% CS (in)	Deflection @ 40% CS (in)	Deflection @ 60% CS (in)	Deflection @ 80% CS (in)
0	0	0	0	0
1	0.266	0.338	0.414	0.476
2	0.270	0.346	0.424	0.488
4	0.278	0.348	0.430	0.494
8	0.282	0.356	0.434	0.504
16	0.282	0.360	0.438	0.504
32	0.284	0.362	0.440	Failed
64	0.288	0.368	0.448	Failed
128	0.292	0.370	0.450	Failed
256	0.294	0.376	0.456	Failed
512	0.298	0.378	0.466	Failed
720	0.302	0.384	0.472	Failed

Table 4.5: Deflection versus time at various constant loads for box B at standard conditions

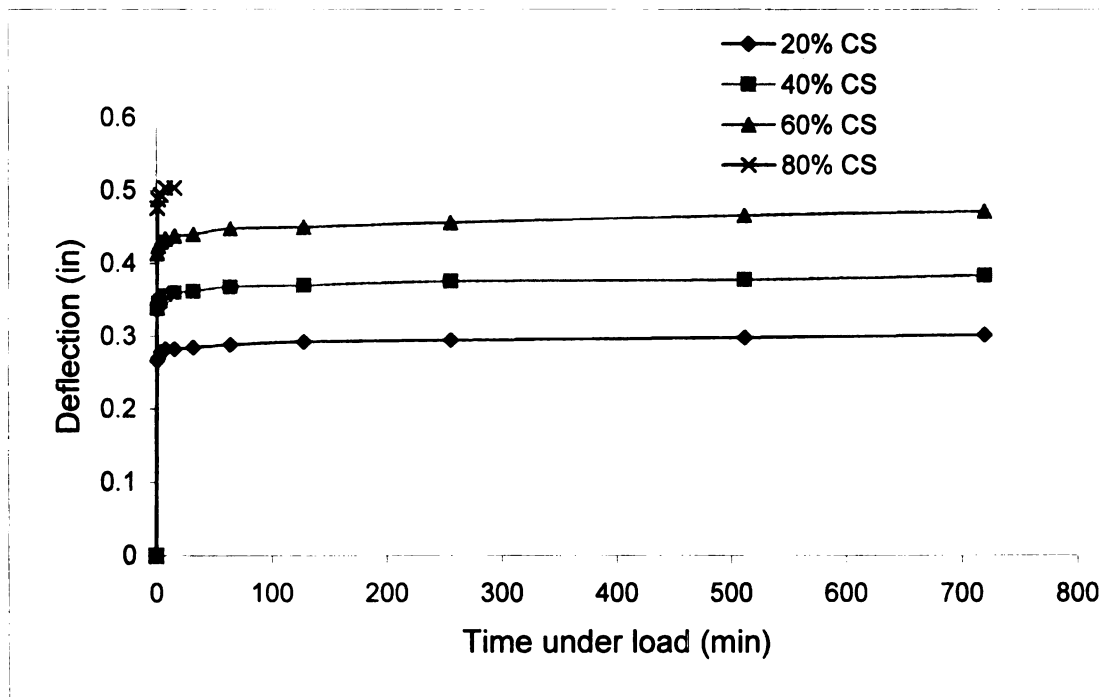


Figure 4.7: Graph of deflection versus time under load at various constant loads for box B at standard conditions

Time (min)	Deflection @ 20% CS (in)	Deflection @ 40% CS (in)	Deflection @ 60% CS (in)	Deflection @ 80% CS (in)
0	0	0	0	0
1	0.250	0.300	0.370	0.390
2	0.256	0.310	0.380	0.418
4	0.258	0.316	0.386	0.440
8	0.260	0.320	0.388	0.466
16	0.266	0.324	0.390	0.480
32	0.268	0.328	0.394	Failed
64	0.268	0.328	0.396	Failed
128	0.270	0.330	0.400	Failed
256	0.274	0.334	0.404	Failed
512	0.280	0.338	0.408	Failed
720	0.282	0.340	0.410	Failed

Table 4.6: Deflection versus time at various constant loads for box B at 80°F, 80%RH

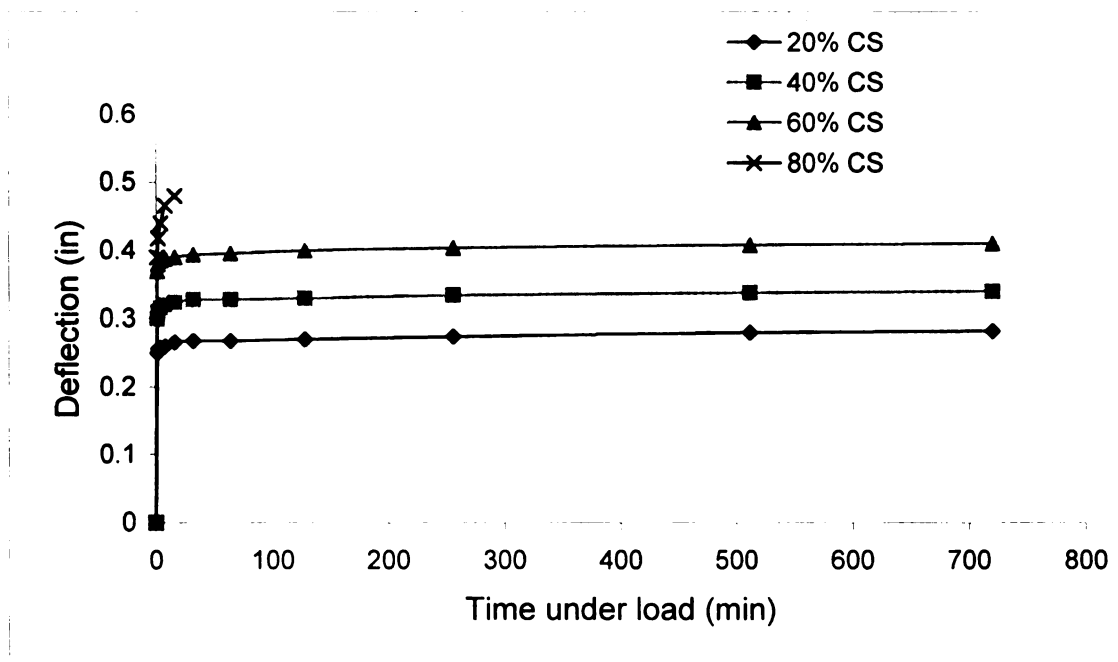


Figure 4.8: Graph of deflection versus time under load at various constant loads for box B at 80°F, 80%RH

### 4.3 Dead Load Tests (Sand Bag Tests)

The test boxes were checked for failure every half an hour for the first 6 hours, and after 24 hours. These actual times to fail are averages over two replicates. The times to collapse are shown in Tables 4.7 and 4.8.

Load (%CS)	Actual time (Standard Conditions)	Actual Time (80°F,80%RH)
20%	over 6 weeks	over 6 weeks
40%	14 days	12 days
60%	2 days	2 days
80%	0.5 hours	0.5 hours

**Table 4.7: Actual times to fail of box A at various constant top loads and storage conditions**

Load (%CS)	Actual time (Standard Conditions)	Actual Time (80°F,80%RH)
20%	over 6 weeks	over 6 weeks
40%	8 days	12 days
60%	3 days	3 days
80%	0.5 hours	0.5 hours

**Table 4.8: Actual times to fail of box B at various constant top loads and storage conditions**

The test boxes are shown in Figure 4.9 below. It is noted that the plywood has tilted to one side, indicating that either the load was not centered over the box, or the box was weaker on one side, or both.

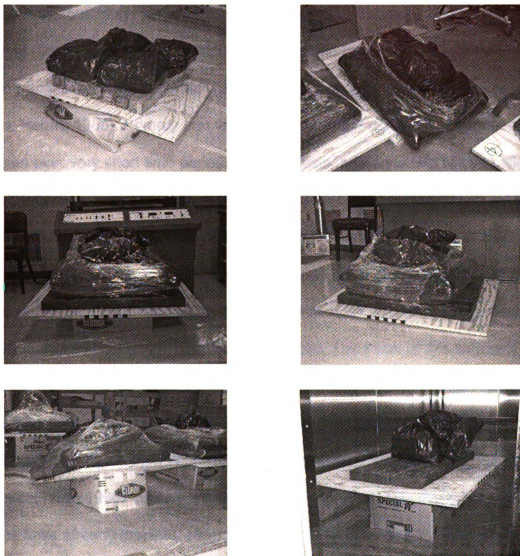


Figure 4.9: Dead load test

## 5. DISCUSSION

### 5.1 Creep in Corrugated Boxes

Creep is the relationship between the deformation of the material versus time under load while the material is subjected to prolonged constant loading. Creep in various materials is different since materials behave differently under loading. Creep of all materials including corrugated boxes can be divided into three regions: primary, secondary and tertiary creep (Moody and Skidmore, 1966; Hearn, 1985). Primary and tertiary creep are not really creep because they happen over very short time periods. In this thesis, primary creep will be called initial deflection: secondary creep will be called creep and tertiary creep will be called failure. The general form of deflection versus time under load or creep curve of corrugated boxes is shown in Figure 5.1. Initial deflection starts at a rapid rate in the first minute of loading and slows down with time. Creep has a slowly increasing deflection over time under load. The slope of this segment is called creep rate. This creep could take days, months or even years, depending on the amount of dead load on the top of boxes. The final is failure where deflection is going up again and results in box failure at this transition (Moody and Skidmore, 1966). Failure will take a couple minutes since the corrugated boxes have already lost their strength and ability to withstand top load when changing from the creep to the failure.

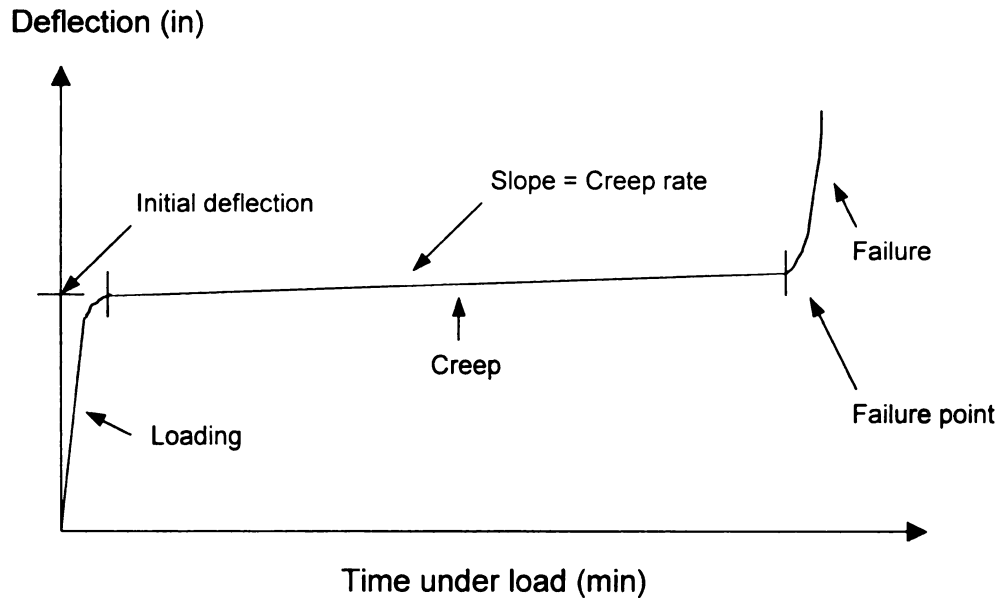


Figure 5.1: Typical creep curve of corrugated boxes under constant load

In the 12-hour creep test, a constant load is set on top of each box using the compression tester as mentioned in section 3.4.2 in Chapter 3. All tested boxes used in this research collapsed in less than 12 hours when the load was equal to 80% of the ASTM D 642 compression strength. If the relationship between deflection and time under load at a top load equal to 80% is plotted on Y and X-axis, the plot will show all three segments as in Figure 5.1. On the other hand, the test results for a top load equal to 20%, 40% and 60%, failure will take longer than 12 hours. Hence, they do not see all three segments because the test was designed to stop at 12 hours. Basically, for a top load equal to 20%, 40% and 60%, only the initial deflection and creep occur within the 12-hour testing period. The data from the 12-hour creep tests (Chapter 4 for boxes A

and B) used in this research at top load equal to 80% of the ASTM D 642 are shown in Tables 5.1, 5.2, 5.3 and 5.4. The creep curves for boxes A and B at a top load equal to 80% are shown in Figures 5.2, 5.3, 5.4 and 5.5.

Time under load (min)	Deflection @ 80% CS (in)
0	0.00
1	0.23
2	0.24
4	0.25
8	0.26
16	0.26
32	0.28
64	0.28
128	0.28

Table 5.1: Deflection versus time under load for box A under constant load equal to 80% of ASTM D 642 at standard conditions

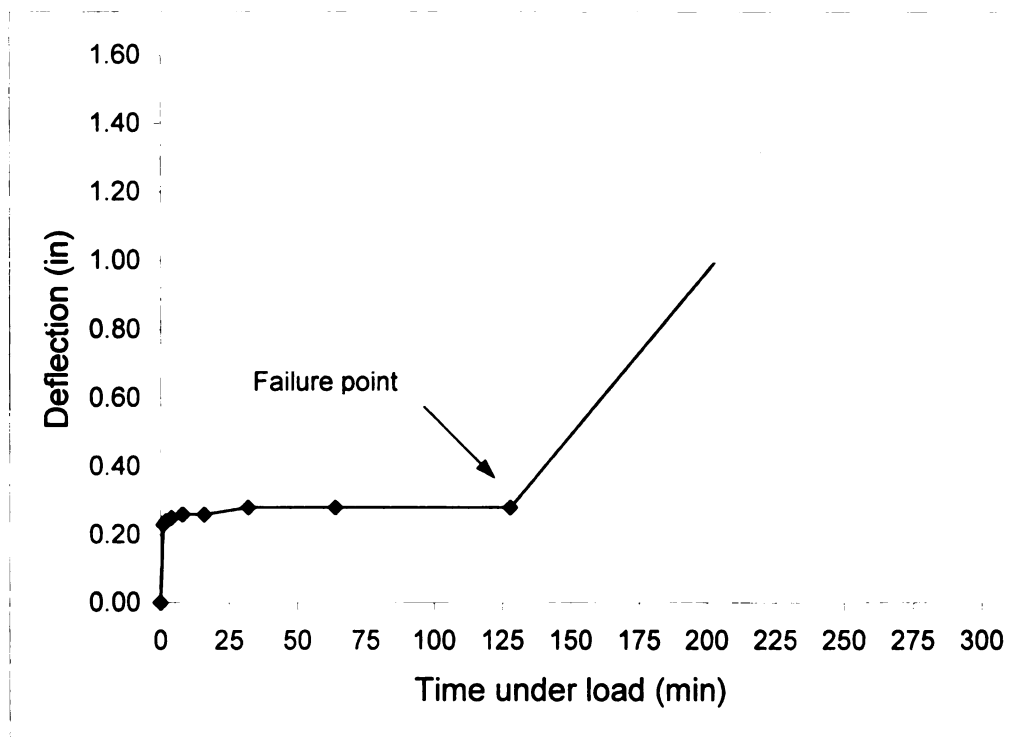


Figure 5.2: Creep of box A under constant load equal to 80% of ASTM D 642 at standard conditions

Time under load (min)	Deflection @ 80% CS (in)
0	0.00
1	0.22
2	0.23
4	0.24
8	0.25
16	0.25

Table 5.2: Deflection versus time under load for box A under constant load equal to 80% of ASTM D 642 at 80°F, 80%RH

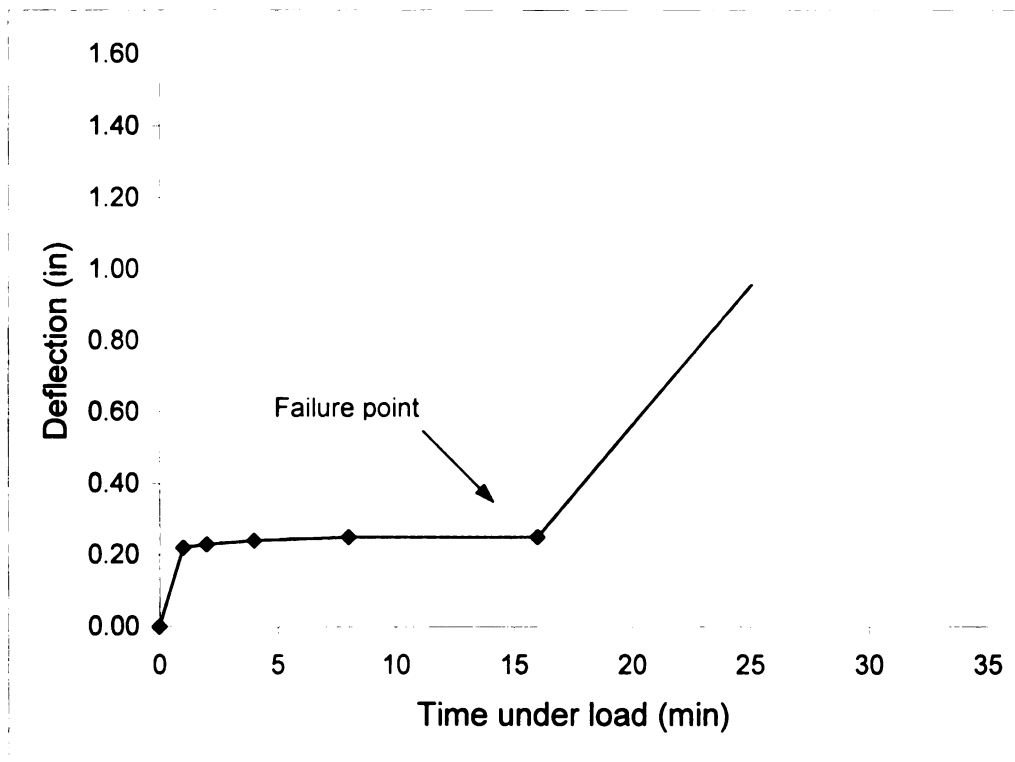


Figure 5.3: Creep of box A under constant load equal to 80% of ASTM D 642 at 80°F, 80%RH

Time under load (min)	Deflection @ 80% CS (in)
0	0.00
1	0.48
2	0.49
4	0.49
8	0.50
16	0.50

Table 5.3: Deflection versus time under load for box B under constant load equal to 80% of ASTM D 642 at standard conditions

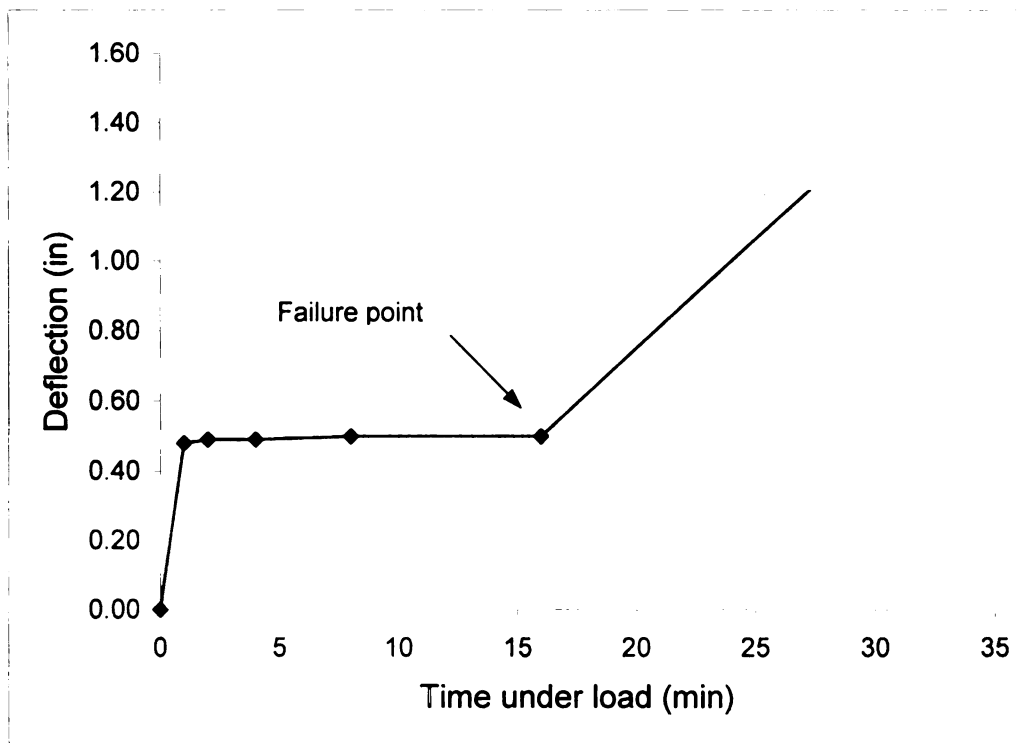


Figure 5.4: Creep of box B under constant load equal to 80% of ASTM D 642 at standard conditions

Time under load (min)	Deflection @ 80% CS (in)
0	0.00
1	0.39
2	0.41
4	0.44
8	0.46
16	0.48

Table 5.4: Deflection versus time under load for box B under constant load equal to 80% of ASTM D 642 at 80°F, 80%RH

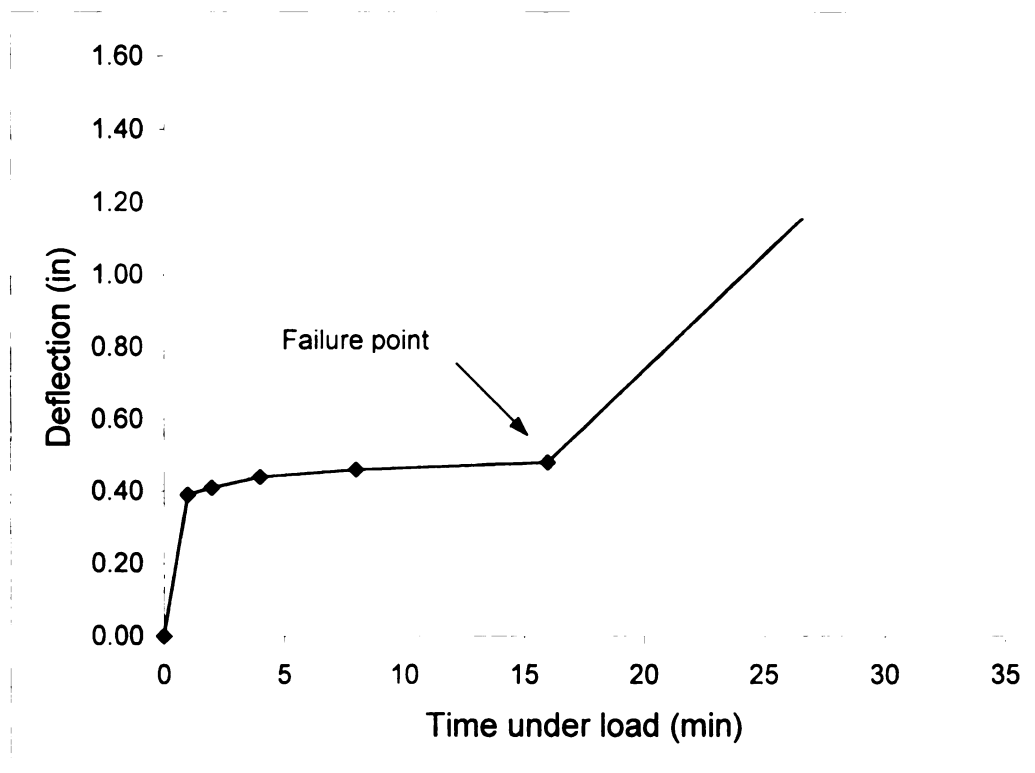


Figure 5.5: Creep of box B under constant load equal to 80% of ASTM D 642 at 80°F, 80%RH

## **5.2 Engineering Failure Analysis**

Materials are classified as ductile or brittle. Ductile materials can be subjected to a large strain before they rupture. Conversely, brittle materials exhibit little or no yielding before they fail. However, some materials still exhibit both ductile and brittle depending on their structure and the temperature and humidity during the time of test. For example, steel has ductile behavior when it contains low carbon content, and it has brittle property when the carbon content is increased. In general, at low temperature materials tend to be hard and brittle, whereas when temperature goes up they become softer and more ductile.

Corrugated board is considered as a moderately brittle material since it has a quite low percent deflection at any testing conditions before failure. For example, boxes A and B used in this research have 12" and 10" depth, respectively. According to ASTM D 642, the deflections at peak for boxes A and B are 0.28" and 0.50" at standard conditions, respectively. Therefore, the percent deflection at peak for B-flute corrugated board fabricating for box A is  $(0.28/12) \times 100\% = 2.33\%$ . Likewise, percent deflection at peak for the C-flute corrugated board fabricating for box B is  $(0.50/10) \times 100\% = 5.00\%$ . The 2.33% and 5.00% elongation is considered as a brittle material.

The theoretical failure criteria commonly used in engineering failure analysis are based on whether the material is considered ductile or brittle. Brittle materials usually fail whenever the stress or strain on them reaches a certain limit, regardless of how much the material is pre-worked or how long it takes to reach this limit. For ductile materials, this limit can change depending on how the

material is stressed. All of the common failure theories will be evaluated for their ability to predict the corrugated containers' life during static long-term storage.

### **5.2.1 Maximum Stress Failure Criterion**

This theory assumes that when the maximum stress on the corrugated container reaches some critical value, failure occurs. This is equivalent to saying that the container fails whenever the top load on it reaches some critical value. This value would necessarily be the compression strength from ASTM D 642.

This theory can be shown to apply to brittle materials, but there is considerable experimental evidence that the theory should not be applied for ductile materials (Hearn, 1985). This is because ductile materials can withstand different amounts of stress without failure, depending on how the material is worked prior to failure. As mentioned earlier, corrugated board are considered as a brittle material so this theory might have a possibility to predict failure of corrugated containers.

In this research, the compression strength that causes boxes A and B failure can be obtained from ASTM D 642. According to Tables 4.1 and 4.2 in Chapter 4, boxes A and B at standard condition and at 80°F, 80%RH will collapse whenever they experience force equal to their compression strength which are 730 lbs, 595 lbs, 1240 lbs and 985 lbs, respectively. In fact, this is definitely not true.

According to the 12-hour creep tests, if the compression load, which is less than its maximum value, has been placed on top of the box long enough, the corrugated container will fail. For example, a top load equal to 80% of the ASTM D 642 strength can cause corrugated boxes to fail in less than 12 hours. So the boxes can be made to fail at top load level below its compression strength if the

top load is left on long enough. This might be because the corrugated containers tend to creep. This says that maximum stress failure criterion cannot be used for materials which tend to creep. Therefore, it is impossible to model long-term storage of corrugated boxes using the maximum stress failure criterion.

### **5.2.2 Maximum Strain Failure Criterion**

This theory assumes that when the maximum strain on the corrugated container reaches some critical value, failure occurs. This is equivalent to saying that the container fails whenever the deflection reaches some critical value. This value would necessarily be the deflection at failure from ASTM D 642.

According to this criterion, the boxes A and B at standard conditions and at 80°F, 80%RH should collapse whenever they experience deflections equal to their ASTM D 642 failure deflections which are about 0.28" for the box A and about 0.50" for the box B, respectively regardless of the temperature and relative humidity. According to the 12-hour creep tests, at top loads equal to 80% of their ASTM D 642 strengths, the boxes did collapse when their deflections reached their ASTM D 642 failure deflections. This would explain why it is possible to make the boxes fail at loads less than the ASTM D 642 compression strength: the boxes creep slower at smaller loads, but eventually reach the same deflection when they fail.

Consider the ASTM D 642 failure deflection at standard conditions and 80°F, 80%RH of both kinds of boxes, which are 0.28" and 0.25" for the box A, 0.50" and 0.48" for the box B. The failure deflections for each box style are very close. This implies that the same kind of boxes will collapse at the same failure deflection, regardless of what condition they are stored.

According to Appendix A, viscoelastic models can sometimes be used to explain creep behavior. The model will produce a relationship between box deflection and time under load. By setting the box deflection equal to the ASTM D 642 failure deflection, the failure time can be calculated. The form of empirical models is predetermined by considering the distribution of experiment data, a knowledge of mathematics, physics and engineering related to the properties of the material, and even the experience of the modeler. In order to predict the failure time of corrugated boxes, all the experiment data from the 12-hour creep tests is used to construct the model.

Creep rate is needed to calculate time to fail of corrugated boxes. However, it is impossible to have all the creep data up to the entire time to fail in order to calculate the creep rate since the creep test was stopped at 12 hours.

Initial deflection takes place very rapidly in the first minute of loading. Therefore, all the 12-hour creep data right after the first minute of loading are considered to be in the creep region. According to the 12-hour creep tests in Figures 4.5 through 4.8 in Chapter 4, the graphs show the deflection increasing linearly over time under load. The 12-hour creep data is therefore considered to represent the creep data, and they can be used to calculate as a creep rate.

By placing a dead load on top of the box in the sand bag tests, there are two stages involved in the compression process. First, during the loading phase, there would be an initial compression which takes place very quickly. This results in that the box deflection increases rapidly with increasing dead load. This stage is over when the dead load is achieved. Basically, this stage is initial deflection. Therefore, creep takes place after the dead load is achieved. The box will collapse when its deflection reaches its ASTM D 642 failure deflection.

During initial deflection, as the dead load is being placed on top of box, the top load versus box deflection follows the ASTM D 642 curve. The box deflection can be estimated from Figure 5.6. The initial deflection can be expressed as in Eq. (5.1).

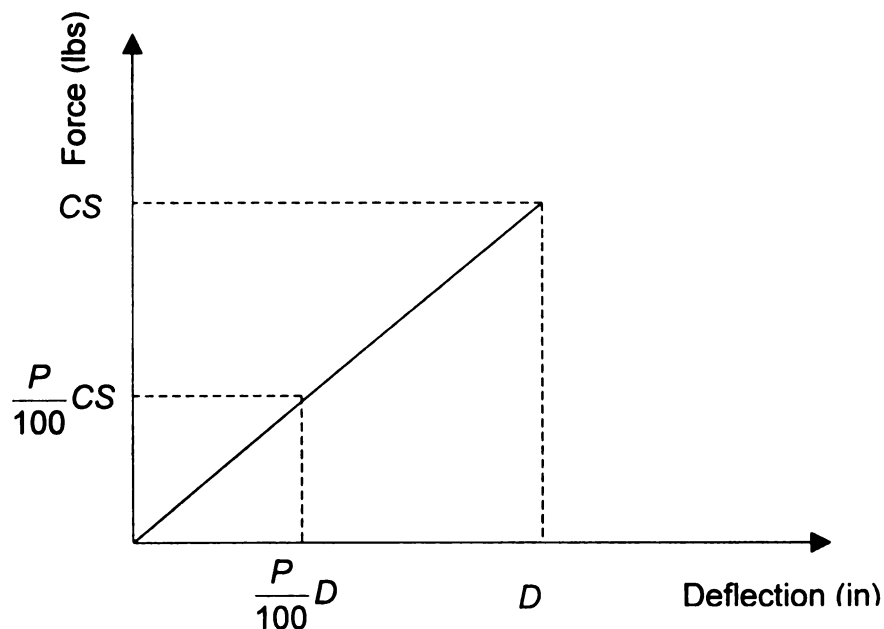


Figure 5.6: ASTM D 642 curve

$$D_i = \frac{P}{100} \times D \quad (5.1)$$

where:

$D_i$  = Initial deflection (in)

$D$  = ASTM D 642 failure deflection (in)

$CS$  = ASTM D 642 compression strength (lbs)

$P$  = Load level expressed as a percent of compression strength

During creep, the additional deflection can be calculated as the product of the creep rate and the time under load (time to fail) as expressed in Eq. (5.2).

The creep rate can be obtained from the computer program written in BASIC (see Appendix B) by using the 12-hour creep data for the particular box style, load level and storage conditions. Linear regression was used in the computer program. The starting data point should correspond to the time that creep begins, which is about at the first minute.

$$D_c = R_{12} \times T \quad (5.2)$$

where:

$D_c$  = Creep deflection (in)

$R_{12}$  = Creep rate at load level  $P$  (in/min)

$T$  = Time to fail (min)

According to maximum strain failure criterion, the corrugated boxes will fail when the sum of initial deflection and creep deflection is equal to their ASTM D 642 failure deflection. This can be expressed as in Eq. (5.3) and the time to fail can be calculated from Eq. (5.4).

$$\frac{P}{100} \times D + R_{12} \times T = D \quad (5.3)$$

$$T = \frac{D}{R_{12}} \times \frac{(100 - P)}{100} \quad (5.4)$$

where:

T = Time to fail (min)

D = ASTM D 642 failure deflection (in)

R<sub>12</sub> = Creep rate at load level P (in/min)

P = Load level expressed as a percent of compression strength

The creep rate from computer program, the predicted time to fail calculated from Eq. (5.4) and actual time to fail from sand bag tests are shown in Tables 5.5, 5.6, 5.7 and 5.8.

Load (%CS)	ASTM D 642 failure def., D (in)	R <sub>12</sub> (in/min)	Predicted time to fail (strain)	Actual time to fail (Sand bag tests)
20%	0.28	1.92 x 10 <sup>-5</sup>	8.1 days	over 6 weeks
40%	0.28	2.23 x 10 <sup>-5</sup>	5.2 days	14 days
60%	0.28	3.35 x 10 <sup>-5</sup>	2.3 days	2 days
80%	0.28	3.28 x 10 <sup>-4</sup>	2.8 hours	0.5 hours

Table 5.5: Creep rate, predicted and actual times to fail at various constant loads for box A at standard conditions

Load (%CS)	ASTM D 642 failure def., D (in)	R <sub>12</sub> (in/min)	Predicted time to fail (strain)	Actual time to fail (Sand bag tests)
20%	0.25	2.34 x 10 <sup>-5</sup>	5.9 days	over 6 weeks
40%	0.25	2.33 x 10 <sup>-5</sup>	4.5 days	12 days
60%	0.25	3.51 x 10 <sup>-5</sup>	2 days	2 days
80%	0.25	1.59 x 10 <sup>-3</sup>	0.5 hours	0.5 hours

Table 5.6: Creep rate, predicted and actual times to fail at various constant loads for box A at 80°F, 80%RH

Load (%CS)	ASTM D 642 failure def., D (in)	R <sub>12</sub> (in/min)	Predicted time to fail (strain)	Actual time to fail (Sand bag tests)
20%	0.50	3.71 x 10 <sup>-5</sup>	7.5 days	over 6 weeks
40%	0.50	4.77 x 10 <sup>-5</sup>	4.4 days	8 days
60%	0.50	6.25 x 10 <sup>-5</sup>	2.2 days	3 days
80%	0.50	1.58 x 10 <sup>-3</sup>	1.1 hours	0.5 hours

Table 5.7: Creep rate, predicted and actual times to fail at various constant loads for box B at standard conditions

Load (%CS)	ASTM D 642 failure def., D (in)	R <sub>12</sub> (in/min)	Predicted time to fail (strain)	Actual time to fail (Sand bag tests)
20%	0.48	3.44 x 10 <sup>-5</sup>	7.8 days	over 6 weeks
40%	0.48	3.66 x 10 <sup>-5</sup>	5.5 days	12 days
60%	0.48	3.92 x 10 <sup>-5</sup>	3.4 days	3 days
80%	0.48	5.32 x 10 <sup>-3</sup>	0.3 hours	0.5 hours

Table 5.8: Creep rate, predicted and actual times to fail at various constant loads for box B at 80°F, 80%RH

It can be seen that the predicted times to fail for long-term storage of corrugated boxes based on maximum strain failure criterion, Eq. (5.4), show poor agreement with the actual time to fail. This might be because the maximum strain failure criterion is wrong, even though the boxes did fail at their ASTM D 642 failure deflections at 80% load.

It should be noted that the predicted times in Tables 5.5 through 5.8 are based on the deflection versus time under load obtaining from the 12-hour creep test. It is assumed that the box deflection in the 12-hour creep tests would be the same as the deflection in sand bag tests. In reality, it would however be very difficult to define what the deflection of sand bag is since all the four corners of the test box would be different due to off center of center of gravity of top load.

The predicted time to fail based on maximum strain failure criterion calculated from Eq. (5.4) can be compared with survival time calculated from Eq. (2.5) done by Koning and Stern in 1977 as mentioned in Chapter 2. Eq. (2.5) can again be rewritten as follows:

$$T_{KS} = \frac{4988}{R_{KS}^{1.038}} \quad (5.5)$$

where:

$T_{KS}$  = Duration of load or survival time (hour)

$R_{KS}$  = Creep rate per box depth (in/in/hr x  $10^6$ )

KS = Koning and Stern

Since the power 1.038 in Eq. (5.5) is very close to 1, Eq. (5.5) can be written as:

$$T_{KS} = \frac{4988}{R_{KS}} \quad (5.6)$$

Assuming that the average creep rate  $R_{12}$  from 12-hour creep tests is the average creep rate in Koning and Stern's previous work, the relationship between  $R_{KS}$  and  $R_{12}$  is

$$R_{KS} = \frac{R_{12}}{H} \times 60 \times 10^6 \quad (5.7)$$

where:

H = Box depth (in)

The depth of boxes A and B used in this research are 12" and 10", respectively.

Hence, an average box depth equal to 11" will be used in Eq. (5.7). Substituting Eq. (5.7) in Eq. (5.6) yields:

$$T_{KS} = \frac{4988}{\left(\frac{R_{12}}{11} \times 60 \times 10^6\right)} \text{ hours} \quad (5.8)$$

or

$$T_{KS} = 60 \times \frac{4988}{\left(\frac{R_{12}}{11} \times 60 \times 10^6\right)} \text{ minutes} \quad (5.9)$$

It is noted that the survival time  $T_{KS}$  in Eq. (5.9) is minutes, not hours.

Eq. (5.9) can be rewritten as in Eq.(5.10). This is the predicted survival time obtained from Koning and Stern's previous work in the form of average creep rate  $R_{12}$ .

$$T_{KS} = \frac{0.055}{R_{12}} \quad (5.10)$$

Comparing the predicted time to fail between Eqs. (5.4) and (5.10), it can be seen that the predicted times to fail obtaining from Eq. (5.4) tend to be longer than the predicted times to fail obtaining from Eq. (5.10). They agree when the top load  $P$  is about 80% for box A and 90% for box B. The difference might be because the data from the experiment of Koning and Stern came from different flute types, adhesives and storage conditions. Besides, the Koning and Stern predicted time to fail came from drawing a straight line on a log-log scale graph. Even their correlation coefficient of 0.98 may still contain a large error. Or, it may be because the maximum strain failure criterion is wrong. The predicted time to fail based on the maximum strain energy failure criterion will be considered in the next section.

### **5.2.3 Maximum Strain Energy Failure Criterion**

This theory assumes that failure occurs when the energy absorbed by the corrugated container reaches some critical amount. This value would necessarily be the strain energy that the box absorbs during compression testing according to ASTM D 642.

When external loads are applied to an object, they will deform the object. The work that has been done by the external loads will be absorbed by the container. This can be expressed as

$$\textit{Energy Absorbed} = \textit{Work Done} \quad (5.11)$$

According to ASTM D 642, the plot of the magnitude of top load  $F$  against the deflection  $x$  of the corrugated box can be obtained from the compression tester automatically. It shows a certain load-deformation characteristic of the corrugated box. The typical plot from ASTM D 642 is shown in Figure 5.7.

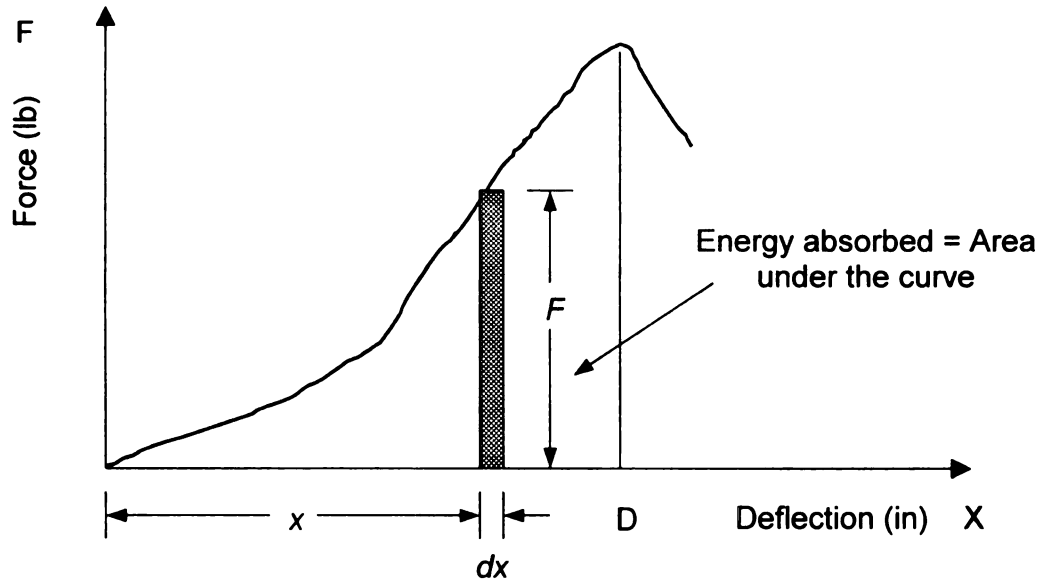


Figure 5.7: Typical graph between force and deflection obtaining from ASTM D 642

Consider the work  $dW$  done by the force  $F$  as the corrugated box deforms by a small amount  $dx$ . This work is equal to the product of the force  $F$  and the small deflection  $dx$ . It can be written as:

$$dW = F \cdot dx \quad (5.12)$$

It should be noted that the expression obtained above is equal to the shadowed area of width  $dx$  located under the graph between force and deflection obtaining from ASTM D 642. The total work done by the top load as the corrugated box deforms a peak deflection  $D$  is thus:

$$W = \int_0^D F \cdot dx \quad (5.13)$$

where:

$W$  = Total work done by top load (in.lb)

$F$  = Top load acting on top of corrugated box (lb)

$D$  = Peak deflection corresponding to ASTM D 642 (in)

$dx$  = Small box deflection (in)

This total work done by the top load is also equal to the area under the curve between  $x = 0$  and  $x = D$ . The total work done by the top load as it is slowly applied to the corrugated box must result in the increase of some energy associated with the deformation of the corrugated box,

$$\text{Energy Absorbed} = W = \int_0^D F \cdot dx \quad (5.14)$$

Practically, the energy absorbed can be determined from the area under the curve using the trapezoid rule (Chapra and Canale 1985), which will provide adequate approximation of the area under the curve, especially when the number of trapezoids is large. Theoretically, the more number of trapezoids, the better the approximation value will be.

If the force versus deflection curve behaves in a linear manner, then the top load will be directly proportional to the deflection. In this case, the graph will be a straight line instead of a curve as shown in Figure 5.8.

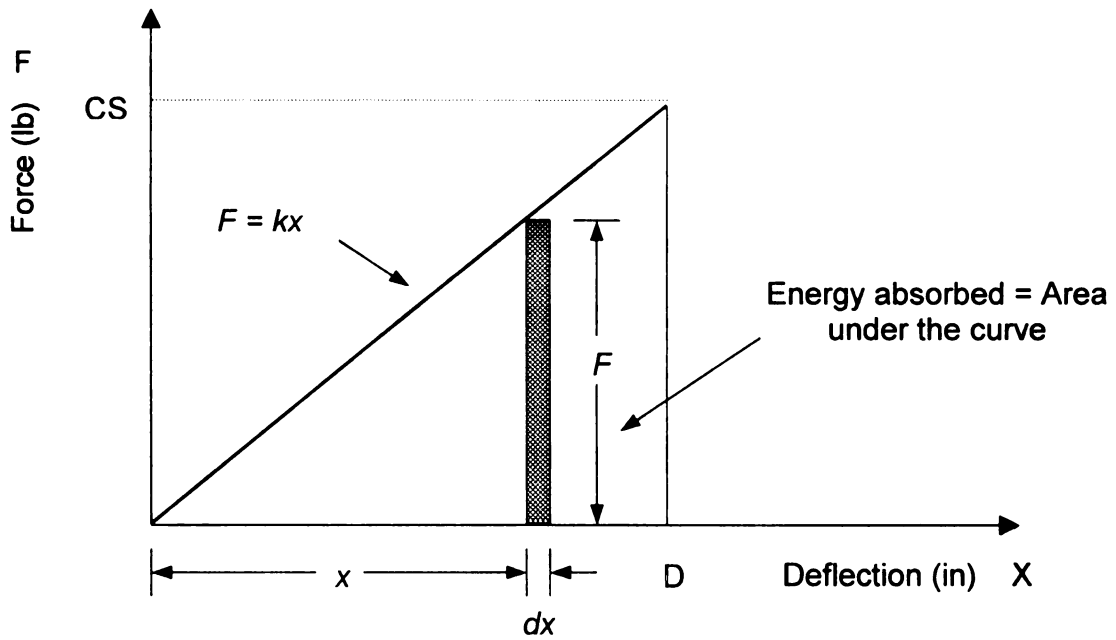


Figure 5.8: Graph between force and deflection of linear material

The equation of the straight line can be written as:

$$F = kx \quad (5.15)$$

where:

$$k = \text{Constant (lb/in)}$$

By substituting Eq. (5.15) in Eq. (5.14), the Eq. (5.14) can be rewritten as the following.

$$\text{Maximum Energy Absorbed} = W = \int_0^D kx \cdot dx = \frac{1}{2}(kD)(D) \quad (5.16)$$

or

$$\text{Maximum Energy Absorbed} = W = \frac{1}{2}(CS)(D) \quad (5.17)$$

where:

CS = Peak force corresponding to ASTM D 642 (lbs)

D = Peak deflection corresponding to ASTM D 642 (in)

Now consider energy absorbed by corrugated containers during long-term storage. The corrugated container absorbs energy by the top load moving down. The corrugated container that is compressed from the top load during sand bag tests has experienced the same phenomena as the simulation tests from 12-hour creep test. Failure occurs when the energy absorbed by the corrugated container during sand bag tests is equal to the energy that the box absorbs during compression testing according to ASTM D 642.

By placing dead load on top of box in the sand bag tests, there are two stages involved in the process, which are initial deflection and creep, as mentioned earlier in section 5.2.2.

During the initial deflection, when the dead load is placed on top of box, the top load versus box deflection follows ASTM D 642 curve. The initial deflection can be estimated from previous Figure 5.6, which is equal to  $\frac{P}{100} \times D$ .

The energy absorbed during the initial deflection, which the corresponding top load equals to  $\frac{P}{100} \times CS$ , can be expressed as in Eq. (5.18).

$$E_i = \frac{1}{2} \left( \frac{P}{100} \times CS \right) \left( \frac{P}{100} \times D \right) \quad (5.18)$$

where:

$E_i$  = Energy absorbed during initial deflection (in.lb)

$D$  = ASTM D 642 failure deflection (in)

$CS$  = ASTM D 642 compression strength (lb)

$P$  = Load level expressed as a percent of compression strength

During creep, the energy absorbed can be calculated from the product of the top load and the creep deflection as expressed in Eq. (5.19). It is noted that the creep deflection is the product of the creep rate and the time to fail as mentioned earlier in Eq. (5.2).

$$E_c = \left( \frac{P}{100} \times CS \right) (R_{12} \times T) \quad (5.19)$$

where:

$E_c$  = Energy absorbed during the creep (in.lb)

$R_{12}$  = Creep rate at load level  $P$  (in/min)

$T$  = Time to fail (min)

According to maximum strain energy failure criterion, the corrugated boxes will fail when the sum of energy absorbed during initial deflection and creep is equal to the energy absorbed up to failure in the ASTM D 642 test. This

can be expressed as in Eq. (5.20) and the time to fail can be calculated from Eq. (5.21).

$$\frac{1}{2} \left( \frac{P}{100} \times CS \right) \left( \frac{P}{100} \times D \right) + \left( \frac{P}{100} \times CS \right) (R_{12} \times T) = \frac{1}{2} (CS)(D) \quad (5.20)$$

$$T = \left( \frac{D}{R_{12}} \right) \left( \frac{50}{P} \right) \left[ 1 - \left( \frac{P}{100} \right)^2 \right] \quad (5.21)$$

where:

D = ASTM D 642 failure deflection (in)

R<sub>12</sub> = Creep rate at load level P (in/min)

P = Load level expressed as a percent of compression strength

T = Time to fail (min)

The creep rates calculated earlier and the predicted times to fail based on the maximum strain energy failure criterion calculated from Eq. (5.21) are shown in Tables 5.9, 5.10, 5.11 and 5.12.

Load (%CS)	ASTM D 642 failure def., D (in)	R <sub>12</sub> (in/min)	Predicted time to fail (strain energy)	Actual time to fail (Sand bag tests)
20%	0.28	1.92 x 10 <sup>-5</sup>	24.3 days	over 6 weeks
40%	0.28	2.23 x 10 <sup>-5</sup>	9.2 days	14 days
60%	0.28	3.35 x 10 <sup>-5</sup>	3.1 days	2 days
80%	0.28	3.28 x 10 <sup>-4</sup>	3.2 hours	0.5 hours

Table 5.9: Creep rate, predicted and actual times to fail at various constant loads for box A at standard conditions

Load (%CS)	ASTM D 642 failure def., D (in)	R <sub>12</sub> (in/min)	Predicted time to fail (strain energy)	Actual time to fail (Sand bag tests)
20%	0.25	2.34 x 10 <sup>-5</sup>	17.8 days	over 6 weeks
40%	0.25	2.33 x 10 <sup>-5</sup>	7.8 days	12 days
60%	0.25	3.51 x 10 <sup>-5</sup>	2.6 days	2 days
80%	0.25	1.59 x 10 <sup>-3</sup>	0.6 hours	0.5 hours

Table 5.10: Creep rate, predicted and actual times to fail at various constant loads for box A at 80°F, 80%RH

Load (%CS)	ASTM D 642 failure def., D (in)	R <sub>12</sub> (in/min)	Predicted time to fail (strain energy)	Actual time to fail (Sand bag tests)
20%	0.50	3.71 x 10 <sup>-5</sup>	22.5 days	over 6 weeks
40%	0.50	4.77 x 10 <sup>-5</sup>	7.6 days	8 days
60%	0.50	6.25 x 10 <sup>-5</sup>	2.9 days	3 days
80%	0.50	1.58 x 10 <sup>-3</sup>	1.2 hours	0.5 hours

Table 5.11: Creep rate, predicted and actual times to fail at various constant loads for box B at standard conditions

Load (%CS)	ASTM D 642 failure def., D (in)	R <sub>12</sub> (in/min)	Predicted time to fail (strain energy)	Actual time to fail (Sand bag tests)
20%	0.48	3.44 x 10 <sup>-5</sup>	23.2 days	over 6 weeks
40%	0.48	3.66 x 10 <sup>-5</sup>	9.6 days	12 days
60%	0.48	3.92 x 10 <sup>-5</sup>	4.5 days	3 days
80%	0.48	5.32 x 10 <sup>-3</sup>	0.3 hours	0.5 hours

Table 5.12: Creep rate, predicted and actual times to fail at various constant loads for box B at 80°F, 80%RH

#### 5.2.4 Strain Energy Criterion – Corrected Creep Rate

The predicted time to fail based on the maximum strain energy failure criterion shows much better agreement with the actual time to fail from sand bag tests than the maximum strain failure criterion as shown in Tables 5.9 through 5.12. It can be concluded that the boxes appear to fail when they absorb a critical amount of energy. Hence, the failure criterion based on maximum strain energy will be chosen as the best predictor and will be further improved as needed.

The predicted time based on maximum strain energy failure criterion does not fit very well with the actual times to fail from sand bag tests for small loads. This might be because the average creep rate  $R_{12}$  is not the appropriate creep rate. In order to better predict failure times for small loads,  $R_{12}$  in Eq. (5.21) will be replaced by a corrected creep rate.

According to the hybrid model (see Appendix A), the average creep rate over the entire time up to failure would be about the same as the creep rate in the 12-hour creep tests if the percent top load  $P$  is very high. This is because the failure times take about 12 hours at very high percent top load. In contrast, if the top load  $P$  is very low, which makes the time under load very long, the creep rate would be about  $\frac{c_1}{(c_1 + c_2)}$  times the creep rate in the 12-hour creep test, where  $c_1$  and  $c_2$  represent the dashpot constants associated with loosely bound and tightly bound pulp respectively (see Appendix A).

Since all previous calculations used the creep rate from the 12-hour creep test as the creep rate over the entire time up to failure, the predicted times based on maximum strain energy failure criterion as shown in Tables 5.9 through 5.12 should be too short for low percent top load P, but the predicted times at high percent top load are right. This is demonstrated in Tables 5.9 through 5.12.

The creep rates in Tables 5.9 through 5.12 should be lower than  $R_{12}$ , especially at low percent top load. According to the hybrid model, the corrected failure times for low percent top load P could be up to  $\frac{c_1 + c_2}{c_1}$  times of the predicted times in Table 5.9 through 5.12 if the creep rates are corrected.

For low percent top load, it makes sense that it would be very difficult to make a long-term prediction accurately by doing a short test for 12 hours. Since we do not want to have the test longer than 12 hours for practical reasons and still want to make a prediction accurately, it is necessary that the creep rate from the 12-hour creep tests be modified.

According to the hybrid model,

$$\text{For } P = 100, \quad R = R_{12} \quad (5.22)$$

$$\text{For } P = 0, \quad R = \frac{c_1}{(c_1 + c_2)} R_{12} \quad (5.23)$$

where:

$R$  = Creep rate over the failure time or Corrected creep rate (in/min)

$R_{12}$  = Creep rate from the 12-hour creep test (in/min)

$c_1$  and  $c_2$  = Dashpot constants (lb.min/in)

Assuming that the relationship between the percent top load  $P$  and the corrected creep rate  $R$  is linear,

$$R = a + bP \quad (5.24)$$

Force-fitting Eq. (5.24) to the condition in Eq. (5.22) and Eq. (5.23) requires that

$$R_{12} = a + b(100) \quad (5.25)$$

$$\frac{c_1}{(c_1 + c_2)} R_{12} = a + b(0) \quad (5.26)$$

Solving Eqs. (5.25) and (5.26) yields:  $a = \frac{c_1}{(c_1 + c_2)} R_{12}$ ,  $b = \frac{c_2}{(c_1 + c_2)} \frac{R_{12}}{100}$

Substituting  $a = \frac{c_1}{(c_1 + c_2)} R_{12}$ ,  $b = \frac{c_2}{(c_1 + c_2)} \frac{R_{12}}{100}$  into Eq. (5.24) yields:

$$R = \frac{R_{12}}{(c_1 + c_2)} \times (c_1 + c_2 \frac{P}{100}) \quad (5.27)$$

Eq. (5.27) gives the corrected creep rate over the entire time up to failure at any load level  $P$ . Using the corrected creep rate instead of the 12-hour creep rate should give more accurate failure times.

Replacing the 12-hour creep rate  $R_{12}$  with the corrected creep rate  $R$  in predicted times based on maximum strain energy failure criterion, Eq. (5.21), yields:

$$T = \left(\frac{D}{R}\right) \left(\frac{50}{P}\right) \left[1 - \left(\frac{P}{100}\right)^2\right] \quad (5.28)$$

Substituting the corrected creep rate  $R = \frac{R_{12}}{(c_1 + c_2)} \times (c_1 + c_2 \frac{P}{100})$  into Eq.

(5.28) yields:

$$T = \frac{D}{R_{12}} \times \frac{(100^2 - P^2)}{2P} \times \frac{1 + \frac{c_1}{c_2}}{P + \frac{c_1}{c_2} 100} \quad (5.29)$$

Since the dashpot constants  $c_1$  and  $c_2$  are not known, a suitable  $\frac{c_1}{c_2}$  ratio can be found by minimizing the sum of squares of errors between the predicted times from Eq. (5.29) and actual times to fail from the sand bag tests. Since the predicted times toward low percent top loads are concerned rather than high percent top loads, only data from top loads equal to 20% and 40% will be used to minimize the sum of squares of errors. Besides, at 20% top load the actual times to fail will be assumed to be 42 days as conservative estimation. The computer program written in BASIC (see Appendix C) gives the least sum of squares of errors when  $\frac{c_1}{c_2} = 0.715$ . If  $\frac{c_1}{c_2} = 0.715$ , Eq. (5.29) can be written as follows:

$$T = 0.857 \times \frac{D}{R_{12}} \times \frac{(100^2 - P^2)}{P(P + 71.5)} \quad (5.30)$$

where:

T = Time to fail (min)

D = ASTM D 642 failure deflection (in)

$R_{12}$  = Creep rate from the 12-hour creep test (in/min)

P = Load level expressed as a percent of compression strength

The corrected creep rates, the predicted times based on Eq. (5.30) and the actual failure times for the boxes A and B are shown in Tables 5.13, 5.14, 5.15 and 5.16.

Load (% CS)	ASTM D 642 failure def., D (in)	$R_{12}$ (in/min)	Predicted time to fail (strain energy)	Corrected R (in/min)	Predicted Time to fail (corrected R)	Actual time to fail (sand bag tests)
20%	0.28	$1.92 \times 10^{-5}$	24.3 days	$1.02 \times 10^{-5}$	45.5 days	over 6 weeks
40%	0.28	$2.23 \times 10^{-5}$	9.2 days	$1.45 \times 10^{-5}$	14.0 days	14 days
60%	0.28	$3.35 \times 10^{-5}$	3.1 days	$2.57 \times 10^{-5}$	4.0 days	2 days
80%	0.28	$3.28 \times 10^{-4}$	3.2 hours	$2.90 \times 10^{-4}$	3.6 hours	0.5 hours

Table 5.13: Corrected creep rates, predicted and actual times to fail of box A at standard conditions

Load (% CS)	ASTM D 642 failure def., D (in)	$R_{12}$ (in/min)	Predicted time to fail (strain energy)	Corrected R (in/min)	Predicted Time to fail (corrected R)	Actual time to fail (sand bag tests)
20%	0.25	$2.34 \times 10^{-5}$	17.8 days	$1.25 \times 10^{-5}$	33.4 days	over 6 weeks
40%	0.25	$2.33 \times 10^{-5}$	7.8 days	$1.51 \times 10^{-5}$	12.0 days	12 days
60%	0.25	$3.51 \times 10^{-5}$	2.6 days	$2.69 \times 10^{-5}$	3.4 days	2 days
80%	0.25	$1.59 \times 10^{-3}$	0.6 hours	$1.40 \times 10^{-3}$	0.7 hours	0.5 hours

Table 5.14: Corrected creep rates, predicted and actual times to fail of box A at 80°F, 80%RH

Load (% CS)	ASTM D 642 failure def., D (in)	$R_{12}$ (in/min)	Predicted time to fail (strain energy)	Corrected R (in/min)	Predicted Time to fail (corrected R)	Actual time to fail (sand bag tests)
20%	0.50	$3.71 \times 10^{-5}$	22.5 days	$1.98 \times 10^{-5}$	42.1 days	over 6 weeks
40%	0.50	$4.77 \times 10^{-5}$	7.6 days	$3.10 \times 10^{-5}$	11.7 days	8 days
60%	0.50	$6.25 \times 10^{-5}$	2.9 days	$4.79 \times 10^{-5}$	3.9 days	3 days
80%	0.50	$1.58 \times 10^{-3}$	1.2 hours	$1.40 \times 10^{-3}$	1.3 hours	0.5 hours

Table 5.15: Corrected creep rates, predicted and actual times to fail of box B at standard conditions

Load (% CS)	ASTM D 642 failure def., D (in)	$R_{12}$ (in/min)	Predicted time to fail (strain energy)	Corrected R (in/min)	Predicted Time to fail (corrected R)	Actual time to fail (sand bag tests)
20%	0.48	$3.44 \times 10^{-5}$	23.2 days	$1.84 \times 10^{-5}$	43.5 days	over 6 weeks
40%	0.48	$3.66 \times 10^{-5}$	9.6 days	$2.38 \times 10^{-5}$	14.7 days	12 days
60%	0.48	$3.92 \times 10^{-5}$	4.5 days	$3.01 \times 10^{-5}$	5.9 days	3 days
80%	0.48	$5.32 \times 10^{-3}$	0.3 hours	$4.70 \times 10^{-3}$	0.4 hours	0.5 hours

Table 5.16: Corrected creep rates, predicted and actual times to fail of box B at 80°F, 80%RH

### **5.3 Errors**

A large error from the new method could possibly come from the uncontrollable location of the center of gravity of the sand bags in the dead load tests. The center of gravity of the sand bags could be positioned at the intersection of box diagonals. In practice, there is no way to know where the center of gravity actually is. If the center of gravity is off positioned, the failure time will be reduced markedly. This is because the plywood placed on top of the box will tilt and start to compress one corner more than the others. The box will therefore collapse sooner. This situation would not happen in the 12-hour creep tests using a fixed platen.

The effect of the center of gravity of the sand bags being off positioned during the dead load tests can be simulated by conducting an additional test using the compression tester with a floating platen. The box B at standard conditions used in this research was tested following ASTM D 642 using the floating platen. The test was designed to place the center of the platen along the box diagonal as shown in Figure 5.9 below. The result showed that the farther the center of the platen along the diagonal is, the less the box compression strength is.

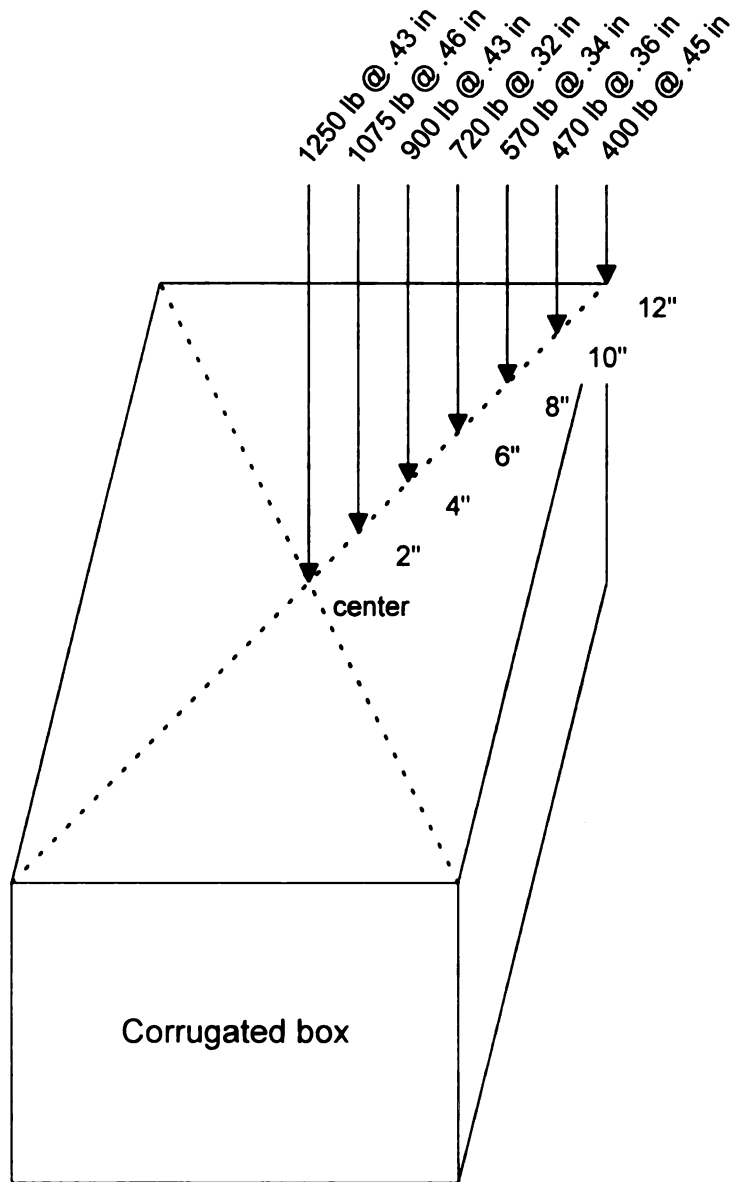


Figure 5.9: Compression strength of box B at different locations along box diagonal following ASTM D642 using floating platen

The realistic placement of sand bags on plywood makes the center of gravity of the sand bags 2 inches off positioned. This will reduce the compression strength of box of  $\frac{1250 - 1075}{1250} \times 100 = 14\%$ . The box will retain 86% of its compression strength. Take 60% compression strength, which is equal to 750 lb as a test top load. This means the top load is really  $\frac{750}{1075} \times 100 = 70\%$  instead of 60%.

Another large error could come from the consistency of the corrugated boxes. Compression strengths are notoriously variable even for identical high quality production run boxes. This consistency could affect the experimental result enormously. Take the box A at standard conditions as an example. The results of ASTM D 642 for all five replicates are shown in Table 5.17 below.

Replicates	CS (lb)	D (in)
Sample1	721	0.26
Sample2	777	0.27
Sample3	753	0.29
Sample4	693	0.27
Sample5	710	0.29
Average	730	0.28
Std.Dev	34	0.01
% Std.Dev	5	5

Table 5.17: ASTM D 642 of box A at standard conditions

The predicted failure times based on Eq. (5.30) and the average compression strength and failure deflection in ASTM D 642 are shown in Table 5.18 below.

Load (%CS)	Predicted time to fail (corrected R)	Actual time to fail (Sand bag tests)
20% (146 lb)	45.5 days	over 6 weeks
40% (292 lb)	14.0 days	14 days
60% (438 lb)	4.0 days	2 days
80% (584 lb)	3.6 hours	0.5 hours

Table 5.18: Actual versus predicted times to fail at various constant top loads of box A at standard conditions

If one wants to test the sensitivity of the predicted times in Table 5.18 to variations in CS and D, this can be done by using extreme values for CS and D from Table 5.17 in Eq. (5.30). Take 60% compression strength, which is equal to 438 lb as a test top load. One never knows what exact compression strength of the new test box is. According to Table 5.17, the box compression strength can be as low as 693 lb or as high as 777 lb. This means that the top load used in the 12-hour creep tests could have actually been between  $\frac{438}{777} = 56\%$  and

$\frac{438}{693} = 63\%$  instead of 60%, as was assumed in Eq. (5.30). By interpolating

Table 5.18, the actual time to fail could therefore vary from 1 day to 9 days

instead of 2 days. Considering that these boxes A used in this research are high quality production run boxes with only 5% standard deviation, the error from the actual time to fail could be up to 450%.

If the errors from the off position of center of gravity of sand bags and the consistency of the corrugated boxes are combined together, the possible

maximum load could be  $\frac{438}{693} \times \frac{1}{86\%} = 73\%$ . By interpolating Table 5.18, the

actual time to fail could be 10 hours instead of 2 days.

The dead load tests were performed using floating platen. This is what corrugated boxes experience in a warehouse. In contrast, the simulation (12-hour creep tests) was performed using fixed platen. This is because it is repeatable and controllable process. The error might come from the difference of using floating and fixed platen.

The test boxes were put in plastics bags during the 12-hour creep test in order to maintain moisture of corrugated board. The plastics bags might create restriction or constrain at the contact surfaces of compression tester platen and top box panel. This did not happen with the contact surfaces of plywood and top box panel in the dead load test.

The variation of temperature and relative humidity in conditioning room could be another source of the error.

More error comes from the recorded times to fail from the sand bag tests. The test boxes were checked for failure every a half an hour for the first 6 hours and every day thereafter. This will result in the error of time to fail by plus a half an hour for 80% top load, and by plus a day for 20%, 40% and 60% top loads.

For example, if a test box with 40% of load on top of it fails at day 14, the box might actually fail at any time between day 13 and day 14.

## **6. CONCLUSIONS**

The results of this research have contributed to packaging in the area of corrugated shipping containers by proposing a new method in order to predict failure times under constant top load in long-term storage of corrugated boxes.

The published retention strength factors done decades ago are too general, meaning that they do not mention box style and what kind of corrugated board the box is made from. Most importantly, they greatly over estimate box endurance. This could be because of the use of recycled paper these days. This results in boxes weaker than before, and also the process of making corrugated boxes has been changed since then.

New strength retention factors can be re-calculated using sand bag tests but the data will also eventually be useless since it will be used specifically only with that box style and material used. The obtained data should not be used to predict failure times of another kind of box style and material used since the failure time would not be accurate. If the top dead load for example is set on a corrugated box at very low percent of its ASTM D 642 compression strength, it could take years to see the box collapsed. The top load equal to 20% of ASTM D 642 is considered a safe load. Even though the results can only be used specifically for that box style and material used, the technique can be used for other boxes.

The new method presented here together with the mathematical model offer an idea that can be used to predict failure time of boxes based on 12-hour

creep tests instead of published retention factors. This offers space and time saving. In order to predict the failure time of corrugated boxes, the test would take only about 12 hours instead of the years it would take to produce new strength retention data. The predicted times show a marked improvement compared to the old published data. A drawback of this new method is that it requires a compression tester. However, the new test method can be performed without compression tester by using some sand bags for top dead load, a ruler and a clock instead of using a compression tester. Doing so will not be as accurate as using a compression tester. Nowadays, compression testers are more and more commonly used in the corrugated box industry, and a small one is considered relatively cheap. Therefore, a compression tester is recommended to do the test.

The new test method can be divided into two parts, testing and working with the mathematical model. First, a corrugated box is compression tested following ASTM D 642. The box compression strength and corresponding failure deflection are recorded. Secondly, a new identical box is compressed at constant load, which is some chosen percentage of its compression strength obtained from ASTM D 642 in the first step. This second test is called creep test and would be performed for 12 hours, which is a realistic limit for industry practice. Deflection versus time is recorded for this percent top load. The duration of 12 hours for the creep test would be recommended for the boxes used in this research, and this should be applied for other similar box styles and material used as well. Finally, the mathematical models based on the maximum strain

energy failure criterion (Eq. (5.30)) along with the data from the ASTM D 642 tests and 12-creep tests are used to calculate the predicted time to fail.

The analysis shows that the mathematical model based on maximum strain energy failure criterion shows a better prediction than a mathematical model based on maximum strain failure criterion. The mathematical model based on strain energy failure criterion using the corrected creep rate would give the best prediction. According to predicted times to fail, it can be concluded that corrugated boxes fail when they absorb a critical amount of energy, which is equal to the energy absorbed on the ASTM D 642 tests.

## **APPENDICES**

**APPENDIX A**  
**VISCOELASTIC MODELS**

In this section, viscoelastic models will be proposed to explain creep behavior. The models could be used to calculate failure time. In order to calculate failure time, box deflection could be set equal to the ASTM D 642 failure deflection. Then, the time under load in the equation could be solved as the failure time.

For years, mechanics of deformable materials has been based on Hooke's law because it is an important assumption in linear elasticity. The force is assumed to have a linear relationship with deflection. When a force is applied to the material, the deflection increases, and when the force is removed the material returns to its original shape. In reality, it has been known that most materials do not behave this way, especially when creep is involved.

In the case of creep, the theory of viscoelasticity has been introduced and applied to the problem. The viscoelastic behavior is a combination of elastic and viscous characteristics of material. No real material obeys either ideal elastic or ideal viscous behaviors, but it is likely between those behaviors. The viscoelastic equations may be either linear or nonlinear. However, the theory of linear viscoelasticity is considered to be a reasonable approximation for real materials like metals at elevated temperature, plastics, concrete, wood, and soil (Flügge, 1967). The linearity still allows the analysis to be less complex with sufficiently rational predictions.

The behavior of viscoelastic material under force can be built from elastic and viscous elements. Springs and dashpots will be used to represent the ideal elastic and viscous behaviors of viscoelastic materials, respectively.

Consider a spring as shown in Figure A1. When a force  $F$  is applied, the length of the spring increases by an amount  $x$ , and when the force is removed the spring returns to its original length. If it is a linear spring, Hooke's law can be applied. The relationship between force  $F$  and the displacement  $x$  can be expressed as in Eq. (A1).

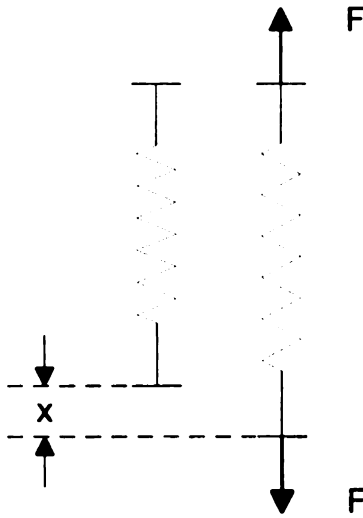


Figure A1: Spring in tension

$$F = kx \quad (A1)$$

where:

$k$  = Constant (spring constant) (lb/in)

Now consider a dashpot as shown in Figure A2. A dashpot is like a piston moving in a cylinder with some small holes in the cylinder bottom. Air is moving in when the piston is pulled out. In contrast, when the piston is pushed in, the air will be driven back out of the cylinder. To move the piston, a force  $F$  is required. The stronger the force  $F$  is, the faster the piston will move. If it is linear, the force  $F$  depends only on the speed of compression, not the amount of compression (as with the spring). The relationship can be written as in Eq. (A2).

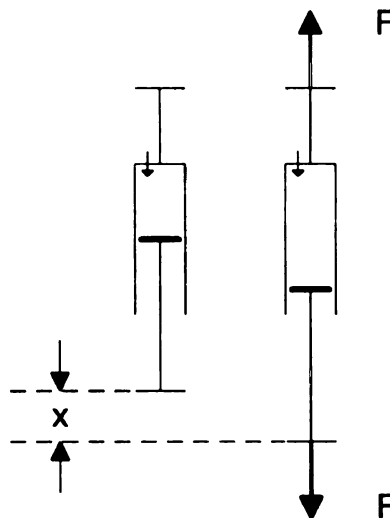


Figure A2: Dashpot in tension

$$F = c \left( \frac{dx}{dt} \right) \quad (\text{A2})$$

where:

$c$  = Constant (dashpot constant) (lb.min/in)

$\frac{dx}{dt}$  = Rate of loading or dashpot compression rate (in/min)

A viscoelastic material can be modeled as a combination of a spring (Hookean solid) and a dashpot (Newtonian fluid) as in Figure A3. Viscoelastic materials show the influence of the rate of loading. The rate of loading depends on force. Moreover, the viscoelastic material can display creep properties, which is an increasing deformation under sustained load.

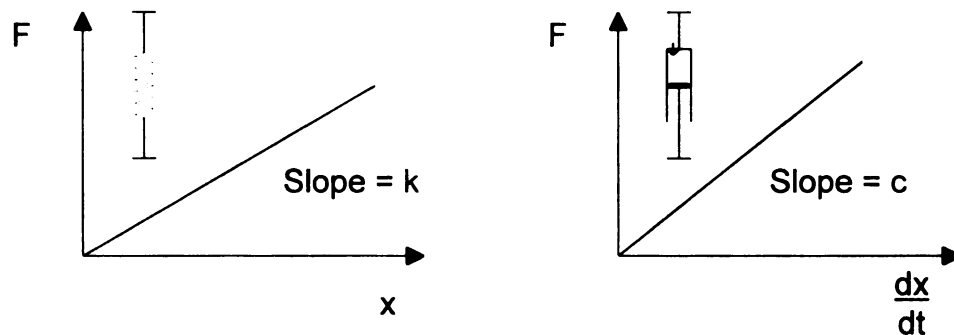


Figure A3: Viscoelastic material modeled by spring (Hookean solid) and dashpot (Newtonian fluid)

In order to describe the behavior of viscoelastic materials, several springs and dashpots can be combined together in a finite network. Theoretically, the network can contain any number of springs and dashpots, and in any configuration to represent the viscoelastic behavior. Practically, it is sometimes too complicated to analyze the model since the model will be composed of many differential equations and variables. The two simplest models of linear viscoelastic material can be obtained by connecting a spring and a dashpot in series and in parallel configurations which are called Maxwell model and Kelvin model, respectively.

## Maxwell Model

The first model representing long-term storage of corrugated box is called Maxwell model. The model is composed of a spring and a dashpot connected together in series as shown in Figure A4.

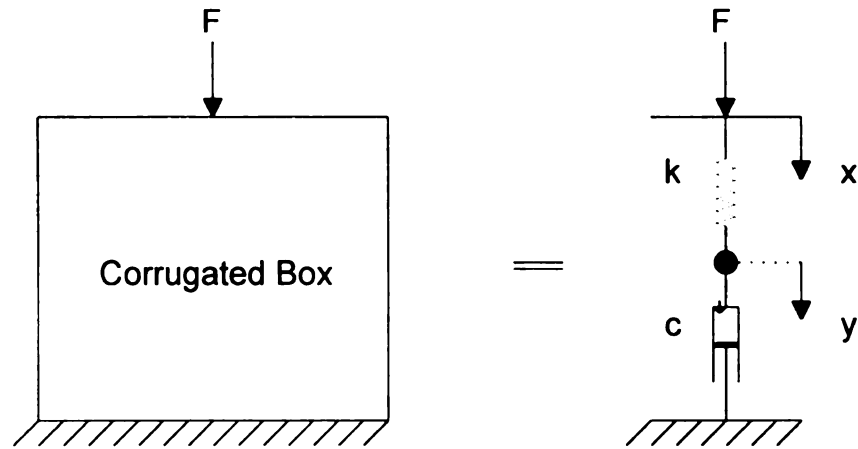


Figure A4: Maxwell model of corrugated box in long-term storage

Consider the Maxwell model in the case when it responds to a constant rate of compression  $v$  as in ASTM D 642. At a constant rate of compression, the top load  $F$  is not constant, but increases with the deflection  $x$ . A balance of forces yields

$$k(x - y) = F \quad (\text{A3})$$

$$c \frac{dy}{dt} = k(x - y) \quad (\text{A4})$$

where:

F = Top load (lbs)

x = Box deflection (in)

y = Deflection (in)

t = Time under load (min)

v = Box compression rate (in/min)

$\frac{dy}{dt}$  = Dashpot compression rate (in/min)

k = Spring constant (lb/in)

c = Dashpot constant (lb.min/in)

Substituting  $x = vt$  in Eq. (A4) and rearranging yields:

$$\frac{dy}{dt} + \frac{k}{c}y = \frac{kv}{c}t \quad (\text{A5})$$

The general solution  $y(t)$  of Eq. (A5) is composed of a complementary solution  $y_c$  and particular solution  $y_p$ . The complementary solution can be solved from  $\frac{dy}{dt} + \frac{k}{c}y = 0$ ; whereas the particular solution can be calculated from

$e^{-\frac{k}{c}t} \int \left( e^{\frac{k}{c}t} \frac{kv}{c} t \right) dt$ . Hence,

$$y_c = Ae^{-\frac{k}{c}t} \quad (\text{A6})$$

$$y_p = e^{-\frac{k}{c}t} \int \left( e^{\frac{k}{c}t} \frac{kv}{c} t \right) dt \quad (\text{A7})$$

$$y_p = \frac{kv}{c} e^{-\frac{k}{c}t} \int \left( e^{\frac{k}{c}t} t \right) dt \quad (\text{A8})$$

Applying integration by parts for  $\int \left( e^{\frac{k}{c}t} \right) dt$  yields:

$$y_p = v\left(t - \frac{c}{k}\right) \quad (\text{A9})$$

Therefore, the general solution  $y(t)$  can be written as follows:

$$y(t) = y_c + y_p \quad (\text{A10})$$

$$y(t) = Ae^{-\frac{k}{c}t} + v\left(t - \frac{c}{k}\right) \quad (\text{A11})$$

Applying the initial condition  $y=0$  at  $t=0$  gives the constant  $A = \frac{cv}{k}$

Substituting  $A = \frac{cv}{k}$  in Eq. (A11):

$$y(t) = vt + \frac{cv}{k}(e^{-\frac{k}{c}t} - 1) \quad (\text{A12})$$

Substituting  $t = \frac{x}{v}$  into Eq. (A12):

$$y(t) = x + \frac{cv}{k}(e^{-\frac{kx}{cv}} - 1) \quad (\text{A13})$$

Substituting Eq. (A13) into Eq. (A3) and rearranging:

$$F(x) = cv\left(1 - e^{-\frac{kx}{cv}}\right) \quad (\text{A15})$$

Consider Eq. (A15) when  $v$  is very large as in the ASTM D 642 tests (0.5 in/min) compared to the creep rate in the 12-hour creep tests. By applying a

Taylor's series expansion, the term  $e^{-\frac{kx}{cv}}$  can be estimated as  $1 - \frac{kx}{cv}$ . Hence, Eq.

(A15) can be rewritten as follows for large compression rates:

$$F(x) = kx \quad (A16)$$

Eq. (A16) is actually the force versus deflection prediction in ASTM D 642 of the Maxwell model. The relationship is a straight line as shown in Figure A5.

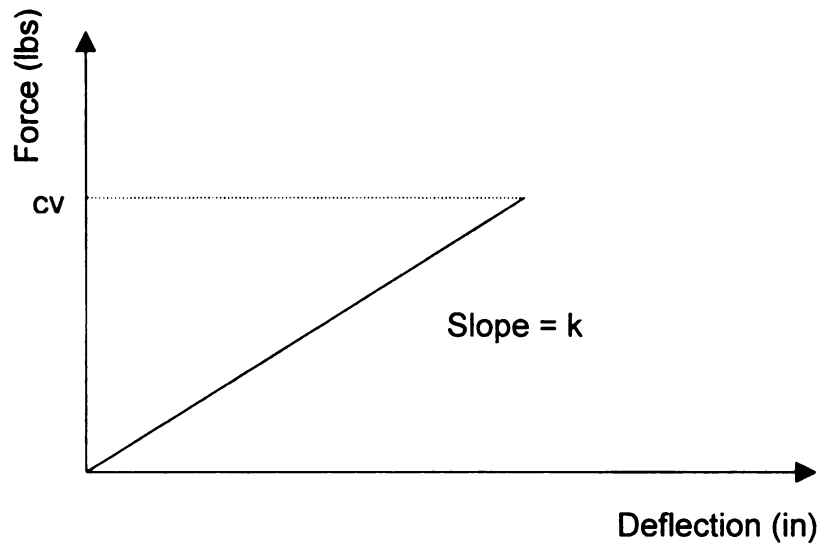


Figure A5: ASTM D 642 of Maxwell model

While the corrugated box is in long-term storage, a different kind of loading occurs. Instead of a constant rate of compression, a constant top load is applied and creep occurs. Now consider Maxwell model in response to a constant weight  $F$ . The relationship between deflection due to creep and time under load is governed by:

$$k(x - y) = F \quad (\text{A.17})$$

$$c \frac{dy}{dt} = F \quad (\text{A.18})$$

Eq. (A18) can be solved as:

$$y(t) = \frac{F}{c}t + A \quad (\text{A.19})$$

Applying the initial condition  $y=0$  at  $t=0$  gives the constant  $A = 0$ .

Substituting  $A = 0$  in Eq. (A19):

$$y(t) = \frac{F}{c}t \quad (\text{A.20})$$

Substituting Eq. (A20) in Eq. (A17) and rewriting:

$$x(t) = \frac{F}{c}t + \frac{F}{k} \quad (\text{A.21})$$

Eq. (A21) predicts that the deflection starts out at  $\frac{F}{k}$  and increases

linearly with slope of  $\frac{F}{c}$  over time under load as shown in Figure A6.

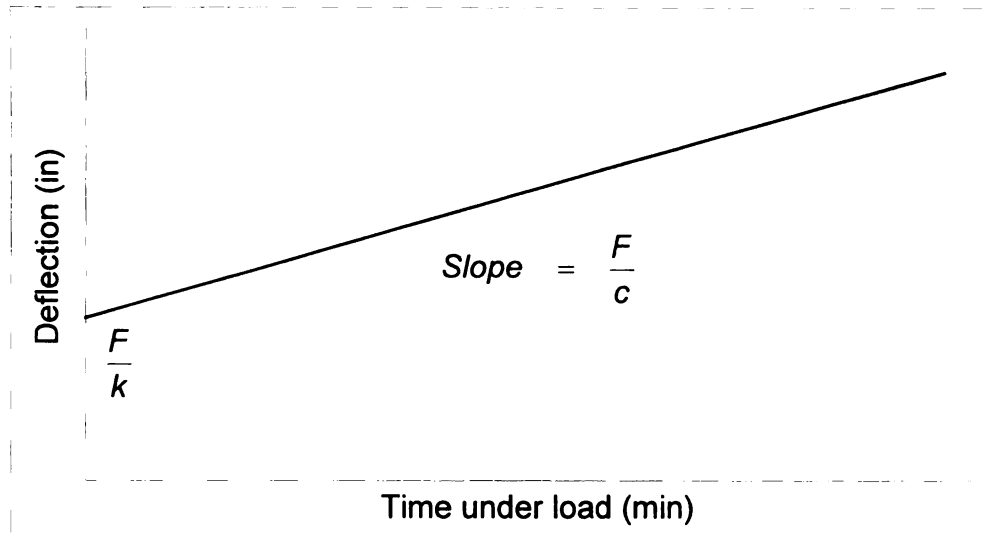


Figure A6: Graph of deflection versus time under load at constant load plotted from Maxwell model

The Maxwell model explains failure region of corrugated boxes under constant load. At time  $t=0$ , the deflection, which is equal to  $\frac{F}{k}$  comes from the spring. Then, the increasing deflection over time comes from the dashpot with the rate of  $\frac{F}{c}$ . Therefore, the failure region occurs due to the effect of the dashpot in the Maxwell model.

The Maxwell model is considered as a bad model since it describes only the failure region of corrugated boxes under constant load. A different model needed in order to describe all three segments.

## Kelvin Model

The next model, called the Kelvin model, is composed of a spring and a dashpot connected together in parallel as shown in Figure A7.

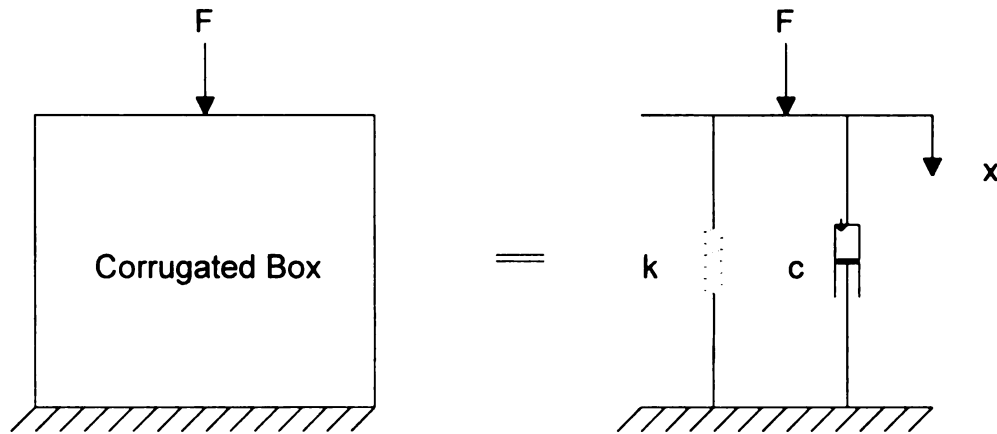


Figure A7: Kelvin model of corrugated box in long-term storage

Consider the Kelvin model in the case when it responds to a constant rate of compression  $v$  as in ASTM D 642. In this case, the top load  $F$  is not constant, but it increases over the deflection  $x$ . Therefore,

$$kx + c \frac{dx}{dt} = F \quad (\text{A22})$$

where:

$F$  = Top load (lbs)

$x$  = Box deflection (in)

$t$  = Time under load (min)

$v$  = Box compression rate (in/min)

$k$  = Spring constant (lb/in)

$c$  = Dashpot constant (lb.min/in)

Substituting  $v = \frac{dx}{dt}$  in Eq. (A22) yields:

$$F(x) = cv + kx \quad (A23)$$

The force versus deflection graph governed by Eq. (A23) still shows a straight line like in ASTM D 642 as shown in Figure A8.

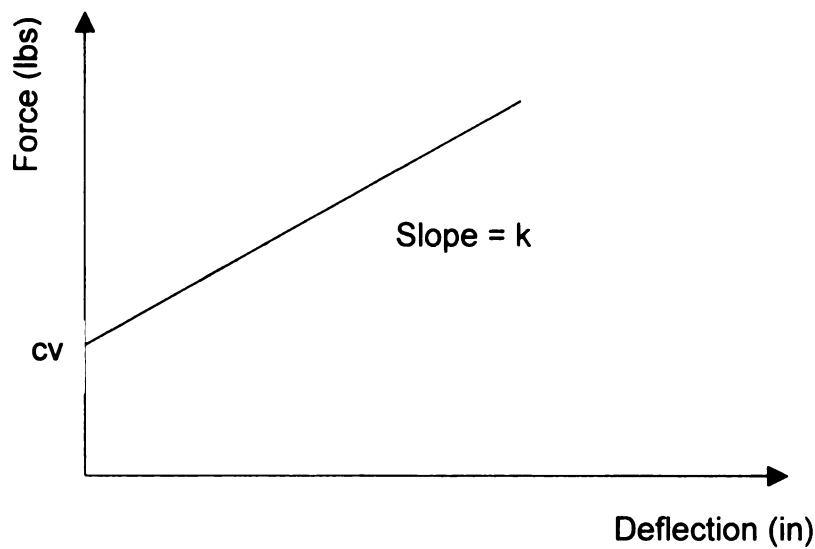


Figure A8: ASTM D 642 of Kelvin model

While the corrugated box is in long-term storage, creep occurs. Now consider the Kelvin model is response to a constant weight  $F$ . The relationship between deflection due to creep and time under load is governed by:

$$kx + c \frac{dx}{dt} = F \quad (\text{A24})$$

The general solution  $x(t)$  of Eq. (A24) is composed of complementary solution  $x_c$  and particular solution  $x_p$ . The complementary solution can be solved from  $\frac{dx}{dt} + \frac{k}{c}x = 0$ ; whereas the particular solution can be calculated from

$e^{-\frac{k}{c}t} \int \left( e^{\frac{k}{c}t} \frac{F}{c} \right) dt$ . Hence,

$$x_c = Ae^{-\frac{k}{c}t} \quad (\text{A25})$$

$$x_p = e^{-\frac{k}{c}t} \int \left( e^{\frac{k}{c}t} \frac{F}{c} \right) dt \quad (\text{A26})$$

$$x_p = \frac{F}{k} \quad (\text{A27})$$

Therefore, the general solution  $x(t)$  can be written as follows:

$$x(t) = x_c + x_p \quad (\text{A28})$$

$$x(t) = Ae^{-\frac{k}{c}t} + \frac{F}{k} \quad (\text{A29})$$

Applying the initial condition  $y=0$  at  $t=0$  gives the constant  $A = -\frac{F}{k}$ .

Substituting  $A = -\frac{F}{k}$  in Eq. (A29):

$$x(t) = \frac{F}{k}(1 - e^{-\frac{k}{c}t}) \quad (\text{A30})$$

Eq. (A30) predicts that the deflection starts out at zero and increases to  $\frac{F}{k}$

exponentially over time as shown in Figure A9.

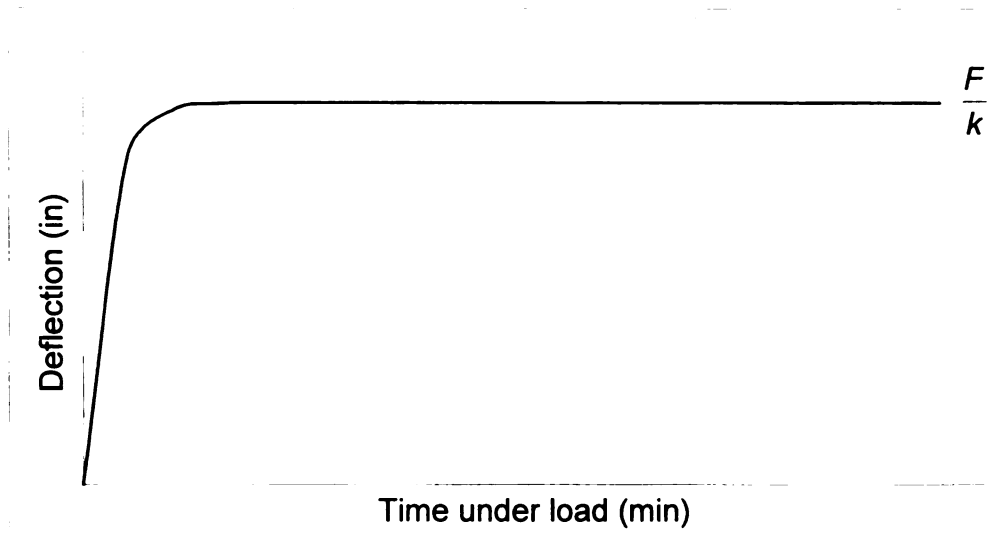


Figure A9: Graph of deflection versus time under load at constant load plotted from Kelvin model

The Kelvin model explains initial deflection and creep of corrugated boxes under constant load. Initial deflection occurs when the dashpot is working very actively to resist the rapidly increasing deflection. The box compression rate is quite large at this stage. The creep starts at the point when the dashpot starts to quit its duty. The spring starts to carry more load since and dashpot carries less load. Eventually, the dashpot totally quits its duty and the spring carries the entire load with the deflection equal to  $\frac{F}{k}$ .

The Kelvin model is also considered as a bad model since it describes only initial deflection and creep of corrugated boxes under constant load. It does not describe failure region. A more sophisticated model is needed. This could be done by combining the properties of the Maxwell and Kelvin models together. A hybrid model will be analyzed next.

## Hybrid Model

The hybrid model is composed of a spring connected in series with a dashpot, and then they connect in parallel with another dashpot as shown in Figure A10. The dashpot on the left hand side acts like loosely bonded pulp in the paper that makes up the corrugated board. The spring and dashpot in series on the right hand side acts like well-bonded pulp inside the paper.

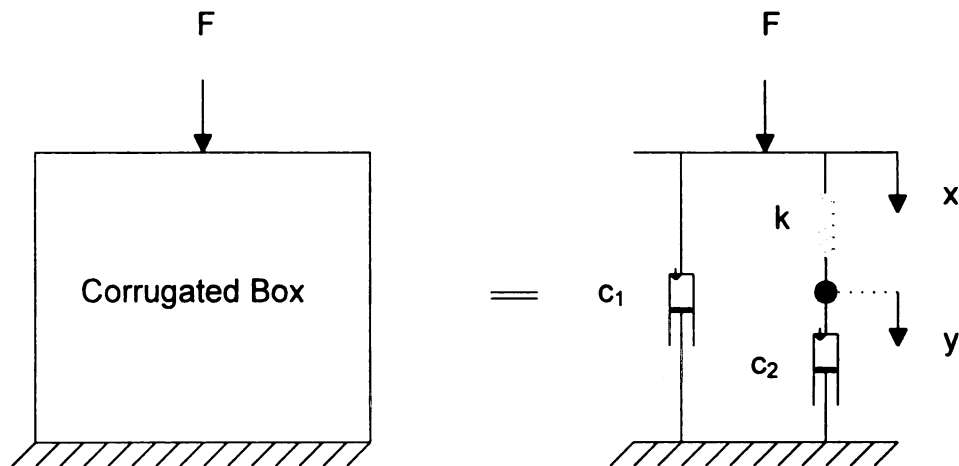


Figure A10: Hybrid model representing long-term storage of corrugated box

Consider the hybrid model in the case when it responds to constant rate of compression  $v$  as in ASTM D 642. In this case, the top load  $F$  is not constant, but increases with the deflection  $x$ . A balance of forces yields:

$$c_1 \frac{dx}{dt} + k(x - y) = F \quad (\text{A31})$$

$$c_2 \frac{dy}{dt} = k(x - y) \quad (\text{A32})$$

where:

F = Top load (lbs)

x = Box deflection (in)

y = Deflection (in)

t = Time under load (min)

v = Box compression rate (in/min)

$\frac{dy}{dt}$  = Dashpot compression rate (in/min)

k = Spring constant (lb/in)

c = Dashpot constant (lb.min/in)

Substituting  $x = vt$  into Eq. (A32) and rearranging:

$$\frac{dy}{dt} + \frac{k}{c_2}y = \frac{kv}{c_2}t \quad (\text{A33})$$

The general solution  $y(t)$  of Eq. (A33) is composed of complementary solution  $y_c$  and particular solution  $y_p$ . The complementary solution can be solved

from  $\frac{dy}{dt} + \frac{k}{c_2}y = 0$ ; whereas the particular solution can be calculated

from  $e^{-\frac{k}{c_2}t} \int \left( e^{\frac{k}{c_2}t} \frac{kV}{c_2} t \right) dt$ . Hence,

$$y_c = Ae^{-\frac{k}{c_2}t} \quad (\text{A34})$$

$$y_p = e^{-\frac{k}{c_2}t} \int \left( e^{\frac{k}{c_2}t} \frac{kV}{c_2} t \right) dt \quad (\text{A35})$$

$$y_p = \frac{kV}{c_2} e^{-\frac{k}{c_2} t} \int \left( e^{\frac{k}{c_2} t} \right) dt \quad (\text{A36})$$

Applying integration by parts for  $\int \left( e^{\frac{k}{c_2} t} \right) dt$  yields:

$$y_p = v \left( t - \frac{c_2}{k} \right) \quad (\text{A37})$$

Therefore, the general solution  $y(t)$  can be written as follows:

$$y(t) = y_c + y_p \quad (\text{A38})$$

$$y(t) = A e^{-\frac{k}{c_2} t} + v \left( t - \frac{c_2}{k} \right) \quad (\text{A39})$$

Applying the initial condition  $y=0$  at  $t=0$  gives the constant  $A = \frac{c_2 V}{k}$ .

Substituting  $A = \frac{c_2 V}{k}$  in Eq. (A39):

$$y(t) = vt + \frac{c_2 V}{k} \left( e^{-\frac{k}{c_2} t} - 1 \right) \quad (\text{A40})$$

Substituting  $t = \frac{x}{v}$  into Eq. (A40):

$$y(t) = x + \frac{c_2 V}{k} \left( e^{-\frac{kx}{c_2 v}} - 1 \right) \quad (\text{A41})$$

Substituting  $v = \frac{dx}{dt}$  and Eq. (A41) into Eq. (A31) and rearranging:

$$F(x) = c_1 v + c_2 v \left( 1 - e^{-\frac{kx}{c_2 v}} \right) \quad (\text{A42})$$

Consider Eq. (A42) when  $v$  is very large as in ASTM D 642. By applying a Taylor's series expansion, the term  $e^{-\frac{kx}{c_2v}}$  can be estimated as  $1 - \frac{kx}{c_2v}$ . Hence,

Eq. (A42) can be rewritten as follows:

$$F(x) = c_1v + kx \quad (A43)$$

Like the Kelvin model, the ASTM D 642 prediction of the hybrid model shows a straight line as shown in Figure A11.

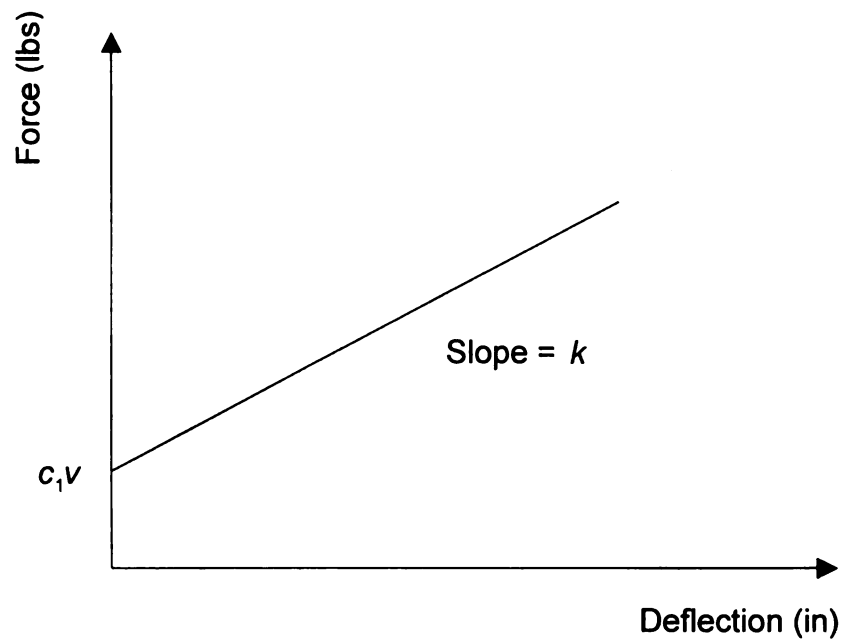


Figure A11: ASTM D642 of hybrid model

While the corrugated box is in long-term storage, creep occurs. Now consider the hybrid model in response to a constant weight  $F$ . The relationship between deflection due to creep and time under load is governed by:

$$c_1 \frac{dx}{dt} + k(x - y) = F \quad (\text{A44})$$

$$c_2 \frac{dy}{dt} = k(x - y) \quad (\text{A45})$$

Define  $D$  is operation  $\frac{d}{dt}$ . Therefore,  $\frac{dx}{dt} = Dx$ .

Applying the operation  $D$  and rearranging Eqs. (A44) and (A45):

$$\frac{c_1}{k} \left( D + \frac{k}{c_1} \right) x - y = \frac{F}{k} \quad (\text{A46})$$

$$-\frac{k}{c_2} x + \left( D + \frac{k}{c_2} \right) y = 0 \quad (\text{A47})$$

Multiply both sides of Eq. (A46) with  $\left( D + \frac{k}{c_2} \right)$  yields:

$$\frac{c_1}{k} \left( D + \frac{k}{c_2} \right) \left( D + \frac{k}{c_1} \right) x - \left( D + \frac{k}{c_2} \right) y = \frac{F}{c_2} \quad (\text{A48})$$

A47 + A48 yields:

$$\frac{c_1}{k} \left( D + \frac{k}{c_2} \right) \left( D + \frac{k}{c_1} \right) x - \frac{k}{c_2} x = \frac{F}{c_2} \quad (\text{A49})$$

$$D \left( D + \frac{k(c_1 + c_2)}{c_1 c_2} \right) x = \frac{kF}{c_1 c_2} \quad (\text{A50})$$

The general solution  $x(t)$  of Eq. (A50) is composed of complementary solution  $x_c$  and particular solution  $x_p$ . The complementary solution can be solved

from  $\frac{d^2x}{dt^2} + \frac{k(c_1 + c_2)}{c_1 c_2} \frac{dx}{dt} = 0$ ; whereas the particular solution can be

calculated from  $\int \left( e^{-\frac{k(c_1 + c_2)t}{c_1 c_2}} \int \frac{kF}{c_1 c_2} e^{\frac{k(c_1 + c_2)t}{c_1 c_2}} dt \right) dt$ . Hence,

$$x_c = A + B e^{-\frac{k(c_1 + c_2)t}{c_1 c_2}} \quad (\text{A51})$$

$$x_p = \frac{F}{c_1 + c_2} \int dt \quad (\text{A52})$$

$$x_p = \frac{F}{c_1 + c_2} t \quad (\text{A53})$$

Therefore, the general solution  $x(t)$  can be written as follows:

$$x(t) = x_c + x_p \quad (\text{A54})$$

$$x(t) = A + B e^{-\frac{k(c_1 + c_2)t}{c_1 c_2}} + \frac{F}{c_1 + c_2} t \quad (\text{A55})$$

$$\frac{dx}{dt} = -\frac{k(c_1 + c_2)}{c_1 c_2} B e^{-\frac{k(c_1 + c_2)t}{c_1 c_2}} + \frac{F}{c_1 + c_2} \quad (\text{A56})$$

Substituting Eqs. (A55) and (A56) into Eq. (A44), and rearranging:

$$y(t) = A - \frac{c_1}{c_2} B e^{-\frac{k(c_1 + c_2)t}{c_1 c_2}} + \frac{F}{c_1 + c_2} t - \frac{c_2 F}{(c_1 + c_2)k} \quad (\text{A57})$$

Applying the initial conditions  $x=0$  and  $y=0$  at  $t=0$  gives

$$A = \frac{c_2^2 F}{(c_1 + c_2)^2 k}, \quad B = -\frac{c_2^2 F}{(c_1 + c_2)^2 k}$$

Substituting  $A$  and  $B$  into Eq. (A55) yields:

$$x(t) = \frac{F}{(c_1 + c_2)} \left[ t + \frac{c_2^2}{(c_1 + c_2)k} \left( 1 - e^{-\frac{k(c_1 + c_2)t}{c_1 c_2}} \right) \right] \quad (\text{A58})$$

Eq. (A58) can be graphed as shown in Figure A12.

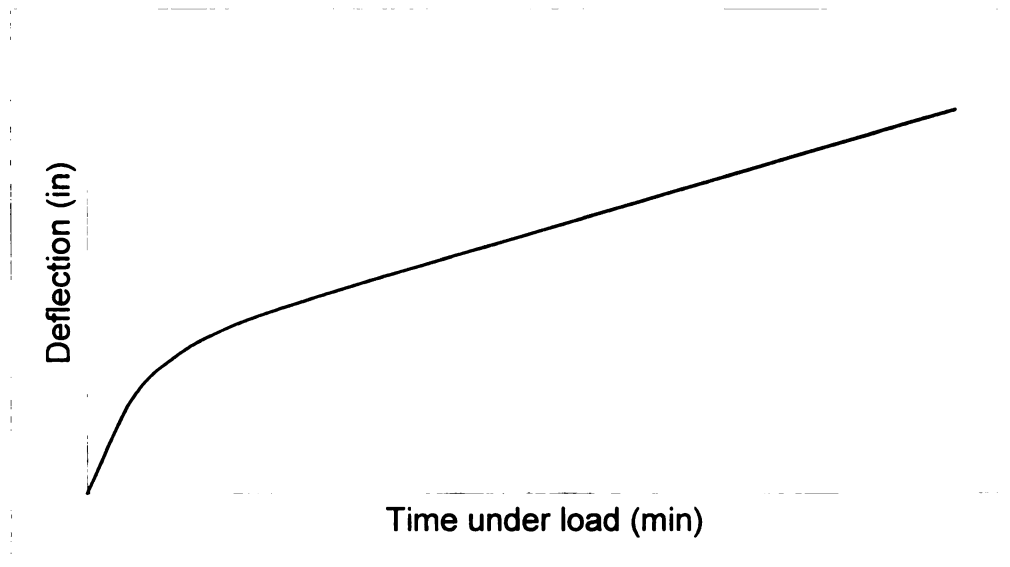


Figure A12: Graph of deflection versus time under load at constant load plotted from hybrid model

The hybrid model tends to show initial deflection and creep but not failure region. The graph shows a long creep region with decreasing creep rate over loading time. This is an important characteristic for predicting long-term storage of corrugated containers. How long boxes can stay in the creep is the most interesting aspect of this research. This is because corrugated containers spend almost all of their lifetime in the creep. With decreasing creep rate over loading time in the hybrid model, this should be a valuable piece of information that can link between short time and long time creep rate.

The average creep rate  $R(t)$  over time under load  $t$  as follows:

$$R(t) = \frac{1}{t} \left[ \int_0^t \left( \frac{dx}{dt} \right) dt \right] \quad (\text{A59})$$

$$R(t) = \frac{1}{t} [x(t)]_0^t \quad (\text{A60})$$

$$R(t) = \frac{x(t) - x(0)}{t} \quad (\text{A61})$$

$$R(t) = \frac{x(t)}{t} \quad (\text{A62})$$

$$R(t) = \frac{F}{(c_1 + c_2)} \left[ 1 + \frac{c_2^2}{(c_1 + c_2)kt} \left( 1 - e^{-\frac{k(c_1 + c_2)t}{c_1 c_2}} \right) \right] \quad (\text{A63})$$

Consider the average creep rate  $R(t)$  in the case when time under load is short as in the 12-hour creep tests. It should note that time under load in the 12-hour creep tests is negligible compared to the sand bag tests. Therefore,

$$R_{12} = \lim_{t \rightarrow 0} R(t) = \frac{F}{(c_1 + c_2)} \left[ 1 + \frac{c_2^2}{(c_1 + c_2)k} \lim_{t \rightarrow 0} \frac{\left( 1 - e^{-\frac{k(c_1 + c_2)t}{c_1 c_2}} \right)}{t} \right] \quad (\text{A64})$$

Since  $\lim_{t \rightarrow 0} \left( 1 - e^{-\frac{k(c_1 + c_2)t}{c_1 c_2}} \right) = 0$  and  $\lim_{t \rightarrow 0} t = 0$ , applying L'Hopital's rule yields:

$$\lim_{t \rightarrow 0} R(t) = \frac{F}{(c_1 + c_2)} \left( 1 + \frac{c_2}{c_1} \right) \quad (\text{A65})$$

$$\lim_{t \rightarrow 0} R(t) = \frac{F}{c_1} \quad (\text{A66})$$

Now consider the average creep rate  $R(t)$  in the case when time under load is very long as in the sand bag tests. The time under load would be considered infinite. Therefore,

$${}_t \lim_{\infty} R(t) = \frac{F}{(c_1 + c_2)} \left[ 1 + \frac{c_2^2}{(c_1 + c_2)k} \lim_{\infty} \frac{(1 - e^{-\frac{k(c_1 + c_2)t}{c_1 c_2}})}{t} \right] \quad (A67)$$

$${}_t \lim_{\infty} R(t) = \frac{F}{(c_1 + c_2)} (1 + 0) \quad (A68)$$

$${}_t \lim_{\infty} R(t) = \frac{F}{(c_1 + c_2)} \quad (A69)$$

Comparing Eqs. (A66) and (A69), it can be concluded that the average creep rate over very long times is  $\frac{c_1}{(c_1 + c_2)}$  times the average creep rate over the 12-hour creep tests. The Maxwell and Kelvin models do not give these characteristics. The relationship can be written mathematically as follows:

$$R_{\text{very long time}} = \frac{c_1}{(c_1 + c_2)} R_{\text{12-hour creep tests}} \quad (A70)$$

Theoretically, a more complicated network composed of many springs and dashpots can be built to better represent the relationship between deflection and time under load of corrugated boxes under constant load. However, it will likely turn out that the model is too complicated to be practical. The biggest problem with this step is how the failure time can be calculated if the spring  $k$ 's and dashpot  $c$ 's constants are not known and they are not easy to find out.

Regardless of how complicated the model is however, an equation similar to Eq. (A70) will result.

**APPENDIX B**  
**CREEP RATE  $R_{12}$**

**THE COMPUTER PROGRAM TO CALCULATE  
CREEP RATE  $R_{12}$**

```
10 REM: FITS STRAIGHT LINE,  $Y=M*X+B$ , TO N (X,Y)'s
20 REM: user makes changes to lines 50 and 60
30 READ N : DIM X(N),Y(N) 'open arrays X and Y for data
40 FOR I=1 TO N : READ X(I),Y(I) : NEXT I 'read N data
50 DATA 11, 1,0.110, 2,0.114, 4,0.114, 8,0.116, 16,0.116, 32,0.116
60 DATA 64,0.118, 128,0.120, 256,0.126, 512,0.126, 720,0.126
70 SX=0 : SY=0 : SXX=0 : SXY=0 : SYY=0 : SSE=0 'initialize sums
80 FOR I=1 TO N 'form sums
90 SX=SX+X(I)/N : SY=SY+Y(I)/N : SXY=SXY+X(I)*Y(I)/N
100 SXX=SXX+X(I)*X(I)/N : SYY=SYY+Y(I)*Y(I)/N
110 NEXT I
120 M=(SXY-SX*SY)/(SXX-SX*SX) : B=SY-M*SX 'slope, y-intercept
130 R=ABS(M)*SQR((SXX-SX*SX)/(SYY-SY*SY)) 'correlation coefficient
140 FOR I=1 TO N : SSE=SSE+(Y(I)-M*X(I)-B)^2 : NEXT I 'sum of squares of
errors
150 PRINT " y=m*x+b fit to";N;"data"
160 PRINT : PRINT " m=";M;" b=";B
170 PRINT : PRINT " x given y predicted y=m*x+b"
180 FOR I=1 TO N : PRINT X(I),Y(I),M*X(I)+B : NEXT I
190 PRINT : PRINT " Creep Rate R12 =" ;M
200 PRINT " correlation coefficient R=" ;R
```

```
210 PRINT " sum of squares of errors SSE=";SSE
```

```
220 PRINT " rms error = sqr(SSE/N)=";SQR(SSE/N)
```

```
230 END
```

**APPENDIX C**  
**CORRECTED PREDICTED TIMES**

**THE COMPUTER PROGRAM TO MINIMIZING DIFFERENCE BETWEEN  
PREDICTED TIMES AND ACTUAL TIMES TO FAIL  
USING SSE TECHNIQUE**

```
10 REM: Minimizing actual and predicted times using SSE technique
20 REM: user makes changes to lines 50,60,70,80,100 and 190
30 READ N : DIM D(N),R12(N),P(N),TA(N) 'open arrays for N data
40 FOR I=1 TO N : READ D(I),R12(I),P(I),TA(I) : NEXT I 'read N data
50 DATA 8, 0.28,1.92E-5,20,42, 0.28,2.23E-5,40,14
60 DATA 0.25,2.34E-5,20,42, 0.25,2.33E-5,40,12
70 DATA 0.50,3.71E-5,20,42, 0.50,4.77E-5,40,8
80 DATA 0.48,3.44E-5,20,42, 0.48,3.66E-5,40,12
90 PRINT" C1/C2 Ratio   SSE": PRINT
100 FOR X= .71 TO .73 STEP .001
110 SSE=0
120 FOR I=1 TO 8
130 TP=D(I)/R12(I)*(100^2-P(I)^2)/(2*P(I))*(1+X)/(P(I)+100*X)/60/24
140 SSE=SSE+(TP-TA(I))^2
150 NEXT I
160 PRINT TAB(3)X, SSE
170 NEXT X
180 PRINT: PRINT"Predicted Times (days)"
190 LET X=.715
200 FOR I=1 TO 8
210 TP=D(I)/R12(I)*(100^2-P(I)^2)/(2*P(I))*(1+X)/(P(I)+100*X)/60/24
```

220 PRINT TP

230 NEXT I

240 END

## **BIBLIOGRAPHY**

## BIBLIOGRAPHY

ASTM Committee D-10 (2003), Selected ASTM Standards on Packaging, 6<sup>th</sup> Edition.

Beldie, L., Sandberg, G., Sandberg, L., Paperboard Packages Exposed to Static Loads-Finite Element Modeling and Experiments, Packaging Technology and Science, Vol. 14, No. 4, 2001.

Buchanan, J.S, Draper, J. and Teague, G.W., Combined Board Characteristics that Determine Box Performance, Paperboard packaging, No. 49, No. 9, September 1964.

Chapra, S.C. and Canale, R.P. (1985), Numerical Methods for Engineers with Personal Computer Applications, McGraw-Hill Book Company, New York.

Fibre Box Association (1994), Fibre Box Handbook, Rolling Meadows, Illinois.

Flugge, F. (1967), Viscoelasticity, Blaisdell Publishing Company, Massachusetts.

Guins, S.G. (1981), Notes on Package Design, 4<sup>th</sup> Edition.

Hearn, E.J. (1985), Mechanics of Materials, 2<sup>nd</sup> Edition, Pergamon Press, Oxford, England.

Kawanishi, K., Estimation of the Compression Strength of Corrugated Fiberboard Boxes and Its Application to Box Design Using a Personal Computer, Packaging Technology and Science, Vol. 2, No. 1, 1989.

Kellicutt, K.Q., Effect of Contents and Load Bearing Surface on Compression Strength and Stacking Life of Corrugated Containers, TAPPI, Vol. 45, 1962.

Koning, J.W. Jr. and Stern, R.K., Long –Term Creep in Corrugated Fiberboard Containers, TAPPI, Vol. 60, No. 12, pp 128-131, December 1977.

Koning, J.W. Jr., Compressive Properties of Linerboard as Related to Corrugated Fiberboard Containers, Theoretical Model Verification, TAPPI, Vol. 61, No. 8, August 1978.

Kutt, H. and Mithel, B. B., Structural and Strength Characteristics of Containers, TAPPI, Vol. 52, No. 9, September 1969.

Maltenfort, G.G., Compression Strength of Corrugated Containers, Paperboard Packaging, Vol. 41, Nos. 7,9,10,11, July, Sept, Oct, Nov 1956.

Maltenfort, G.G., Compression Strength of Corrugated Board, Paperboard Packaging, Vol. 48, No. 8, August 1963.

Maltenfort, G.G., Compression Load Distribution on Corrugated Boxes, Paperboard Packaging, Vol. 65, No. 9, September 1980.

Maltenfort, G. (1989), Performance and Evaluation of Shipping Containers, Jelmar Publishing Company, New York.

Maltenfort, G. (1996), Corrugated Shipping Containers: An Engineering Approach, Revised Edition, Jelmar Publishing Company, New York.

McKee, R.C, Gander, J.W. and Wachuta, J.R., Edgewise Compression Strength of Corrugated Board, Paperboard Packaging, Vol.46, No.11, November 1961.

McKee, R.C, Gander, J.W. and Wachuta, J.R., Flexural Stiffness of Corrugated Board, Paperboard Packaging, Vol.47, No.12, December 1962.

McKee, R.C, Gander, J.W. and Wachuta, J.R., Compression Strength Formula for Corrugated Board, Paperboard Packaging, Vol.48, No. 8, August 1963.

Miller, C. (2002, July 1), Profiles in Garbage: Corrugated Boxes, Wasteage.com [http://wasteage.com/ar/waste corrugated boxes/index.htm](http://wasteage.com/ar/waste%20corrugated%20boxes/index.htm)

Moody, R.C. and Skidmore, K.E., How Dead Load, Downward Creep Influence Corrugated Box Design, Package Engineering, Vol. 11, No. 8, pp 75-81, August 1966.

Peterson, W.S. and Fox, T.S., Workable Theory Proves How Boxes Fail in Compression, Paperboard Packaging, Vol. 65, No. 10, October 1980.

Pommier, J.C., Poustis, J., Fourcade, E., Morlier, P. (1991), Determination of the Critical Load of a Corrugated Cardboard Box Submitted to Vertical Compression by Finite Elements Methods, TAPPI International Paper Physics Conference Proceedings, Book 2 pp.437-448, September.

Rahman, A.A. (1997), Finite Element Buckling Analysis of Corrugated Fiberboard Panels, Mechanics of Cellulosic Materials, pp. 87-92.

Thielert, R., Determination of Stacking Load-Stacking Life Relationship of Corrugated Cardboard Containers, TAPPI, Vol. 67, No. 11, November 1984.

Thielert, R., Edgewise Compression Resistance and Static Load-Lifetime Relationship of Corrugated Board Samples, TAPPI, Vol. 69, No. 1, January 1986.

Thorpe, J.L. and Choi, D., Corrugated Container Failure – Creep Strain Measurements, TAPPI, Vol. 74, No. 10, October 1991.

Thorpe, J.L. and Choi, D., Corrugated Container Failure Part 2 – Strain Measurements in Laboratory Compression Tests, TAPPI, Vol. 75, No. 7, July 1992.

MICHIGAN STATE UNIVERSITY LIBRARIES



3 1293 02504 8194